Slit regulates compartment-specific targeting of dendrites and axons in the *Drosophila* brain

Xiaobing Deng[1], Isaac Cervantes Sandoval[2], Sijun Zhu[1#*]

[1] Department of Neuroscience and Physiology, State University of New York Upstate Medical University, Syracuse, New York 13210, USA

[2]Department of Biology, Georgetown University, Washington D.C., 20057

* Correspondence: zhus@upstate.edu

Lead contact

Running title: Slit regulates compartment-specific targeting of dendrites

Keywords: Slit, Robo, *Drosophila*, dendrites, axons, mushroom body, mushroom body output neurons, dopaminergic neurons, compartment-specific targeting

Abstract

Proper functioning of the nervous system requires precise neuronal connections at subcellular domains, which can be achieved by projection of axons or dendrites to subcellular domains of target neurons. Here we studied subcellular-specific targeting of dendrites and axons in the *Drosophila* mushroom body (MB), where mushroom body output neurons (MBONs) and local dopaminergic neurons (DAN) project their dendrites and axons, respectively, to specific compartments of MB axons. Through genetic ablation, we demonstrate that compartment-specific targeting of MBON dendrites and DAN axons involves mutual repulsion of MBON dendrites and/or DAN axons between neighboring compartments. We further show that Slit expressed in subset of DANs mediates such repulsion by acting through different Robo receptors in different neurons. Loss of Slit-mediated repulsion leads to projection of MBON dendrites and DAN axons into neighboring compartments, resulting formation of ectopic synaptic contacts between MBONs and DANs and changes in olfactory-associative learning. Together, our findings suggest that Slit-mediated repulsion controls compartment-specific targeting of MBON dendrites and DAN axons, which ensures precise connections between MBON dendrites and DAN axons and proper learning and memory formation.

INTRODUCTION

Proper functioning of the nervous system requires neurons to form synaptic contacts not only with correct target cells but also at specific subcellular domains of the target cells (Yogev and Shen 2014). For example, different types of inhibitory GABAergic interneurons in the cerebral cortex form synaptic contacts with excitatory pyramidal neurons at different subcellular domains. Parvalbumin-positive basket cells project their axons to the perisomatic region of pyramidal neurons to form synaptic contacts (Klausberger et al. 2003; Baude et al. 2007), whereas somatostatin-positive interneurons project their axons to distal dendrites of pyramidal neurons (Kawaguchi and Kubota 1997; Wang et al. 2004). In the *Drosophila* ventral nerve cord, it has also been shown that different sensory neurons project their axons to either medial or lateral dendrites of interneurons to form synaptic contacts (Sales et al. 2019; Galindo et al. 2023). Therefore, subcellular specificity of synaptic contacts is a common feature in the nervous system in both invertebrates and vertebrates. The subcellular specificity of synaptic contacts has profound impacts on neuronal activity and computational power of neural circuits (Miles et al. 1996; Pouille and Scanziani 2001).

Mechanisms regulating subcellular specificity of synaptic contacts are still not well understood, but both target cells and non-target cells can regulate targeting of presynaptic axons to specific subcellular domains of target cells. Target cells could regulate targeting of presynaptic axons by expressing cell surface molecules on specific subcellular domains. These cell surface molecules, which can be cell adhesion molecules, receptors, growth factors, etc., guide the projection of presynaptic axons by binding to proteins expressed on the presynaptic axons (Ango et al. 2004; Fazzari et al.

2010; Anderson et al. 2017; Favuzzi et al. 2019; Sando et al. 2019). Non-target cells could also regulate targeting of presynaptic axons. These non-target cells can be neighboring guidepost cells or remote organizers. Non-target cells can express non-diffusible or diffusible guidance molecules to guide the targeting of presynaptic axons to specific subcellular domains of target cells (Colon-Ramos et al. 2007; Ango et al. 2008; Sales et al. 2019). However, the role of non-target cells in regulating subcellular specificity of synaptic contacts is less well studied and the guidance molecules expressed in non-target cells remain to be identified in some cases (Sales et al. 2019; Galindo et al. 2023).

In addition to targeting of presynaptic axons to specific subcellular domains of postsynaptic neurons, subcellular-specific synaptic contacts can also be formed by targeting of postsynaptic dendrites to specific subcellular compartments of presynaptic contacts, but how dendrites are targeted to subcellular domains in presynaptic neurons has rarely been studied. In the *Drosophila* mushroom body (MB), which is an olfactory associative learning and memory center (Guven-Ozkan and Davis 2014; Cognigni et al. 2018), the downstream mushroom body output neurons (MBONs) project their dendrites to specific segments (or compartments) of the MB axonal lobes to form synaptic contacts. MBONs receive synaptic inputs from MB neurons (or called Kenyon cells, KCs) and mediate behavioral outputs (Sejourne et al. 2011; Aso et al. 2014a; Owald et al. 2015; Perisse et al. 2016). There are 34 MBONs of 21 types in each brain hemisphere. Each type of MBONs project their dendrites to 1-2 of a total of 15 compartments in MB axonal lobes that are next to each other without overlap (Fig. 1A) (Tanaka et al. 2008; Aso et al. 2014a). These 15 compartments include 5 in the γ lobe

(right, Fig. 1A), 3 each in the α' and α lobes, and 2 each in the β'and β lobes (Lee et al. 1999). In addition, there are over 100 local dopaminergic interneurons (DANs) of 20 different types, each of which also project their axons to 1-2 compartments in the MB axonal lobes (Tanaka et al. 2008; Aso et al. 2014a). Within each compartment, DAN axons form synaptic contacts with both MB axons and MBON dendrites. DANs modulate synaptic transmission from MB neurons to MBONs and subsequent behavioral outputs in response to different unconditioned stimuli (Schwaerzel et al. 2003; Liu et al. 2012; Aso et al. 2014a; Cohn et al. 2015; Yamagata et al. 2015; Takemura et al. 2017). The DAN axons and MBON dendrites that are targeted to the same compartment have to match exactly for proper behavior outputs. In general, the DANs that are activated by appetitive stimuli form synaptic contacts with MBONs that mediate avoidance behavior, whereas the DANs that are activated by aversive stimuli form synaptic contacts with MBONs that mediate approaching behavior (Schwaerzel et al. 2003; Schroll et al. 2006; Mao and Davis 2009; Liu et al. 2012; Yamagata et al. 2015). Therefore, MBONs and DANs provide an excellent novel model for studying subcellular-specific targeting of dendrites and axons, but how MBONs and DANs project their dendrites and axons to specific compartments and avoid overlapping with those in neighboring compartment remains to be elucidated.

In this study, we investigated cellular and molecular mechanisms regulating compartment-specific targeting of MBON dendrites and DAN axons with a particular focus on those that project their dendrites/axons to the MB γ lobe. By performing a series of genetic ablations, we demonstrate that mutual repulsive interactions, which can be mediated by either MBONs or DANs, between neighboring compartment is

critical to restrict the projection of MBON dendrites and DAN axons to their specific compartments. We identify Slit as a molecule that mediates the repulsion between a subset of compartments, but different MBONs/DANs express different combinations of Robo receptors to mediate the repulsion by Slit. Further, we show that failure to restrict the projection of MBON dendrites to their specific compartments could lead to aberrant synaptic connections between MBON dendrites and DAN axons and subsequent alterations in learning and memory formation.

RESULTS

Compartment-specific targeting of MBON dendrites involves axon- and dendrite-mediated repulsion between neighboring compartments

To investigate mechanisms regulating the compartment-specific targeting of MBON dendrites, we first tried to directly label dendrites of MBONs targeted to individual compartments in the MB γ lobe with alternate fluorescent colors independently of the GAL4-UAS system. To this end, we generated transgenic lines *R27G01-mCD8-GFP*, *R94B10-mCD8-GFP*, *R93D10-mCD8-GFP, and R53C03-CD4-tdTomato*. *R27G01*, *R94B10*, *R93D10,* and *R53C03* are well-characterized enhancer fragments that are active in MBON-γ5β'2a (simplified as MBON-γ5 hereafter), MBON-γ3β'1 (simplified as MBON-γ3 hereafter), MBON-γ1pedc>α/β (simplified as MBON-γ1 hereafter), and MBON-γ4>γ1,γ2 (simplified as MBON-γ4 hereafter) neurons, respectively (Pfeiffer et al. 2008; Jenett et al. 2012). By utilizing these enhancer fragments to directly drive the

expression of mCD8-GFP or CD4-tdTomato, we were able to label MBON-γ5, MBON-γ3, and MBON-γ1 neurons with mCD8-GFP and MBON-γ4 neurons with CD4-tdTomato (Supplemental Fig. S1A-C', E-E'). In addition, we used an existing *R25D01-LexA* line to drive the expression of *LexAop-rCD2-RFP* in MBON-γ2α'1 (simplified as MBON-γ2 hereafter) neurons (Supplemental Fig. S1D-D'). By assembling all these transgenic components together into one fly line, we could simultaneously visualize MBON dendrites targeted to all the five compartments (γ1 through γ5) in the γ lobe with alternate fluorescent colors (Fig. 1B-B"), which allows easy detection of targeting defects of MBON dendrites if any. Furthermore, with these transgenic lines, we could manipulate gene expression in any neurons using the GAL4-UAS system without interfering the visualization of these MBON dendrites.

The compartment-specific targeting of MBON neuron dendrites and DAN axons in the MB axonal lobes could potentially involve attractive interactions between MB axons and MBON dendrites/DAN axons, or between MBON dendrites and DAN axons within individual compartments, and/or repulsive interactions between MBON dendrites and MBON dendrites, between MBON dendrites and DAN axons, or between DAN axons and DAN axons from neighboring compartments. In this study, we tested if compartment-specific targeting of MBON dendrites involves repulsions between neighboring compartments. To this end, we performed systematic genetic ablation of MBONs or DANs that project their dendrites or axons to the MB γ lobe by expressing *UAS-rpr* (*reaper)* and *UAS-hid* (*head involution defective*) (*hid*) together or *UAS-hid*^{Ala5}. Hid^{Ala5} is a mutant Hid in which five amino acid resides of the MAPK phosphorylation

site are changed into Ala residues and can induce cell death efficiently (Bergmann et al. 2002). Meanwhile, we labeled MBONs or DANs that target their dendrites or axons to the neighboring compartments using the transgenic lines we generated or existing LexA lines. Since the γ1 compartment is slightly separated from other compartments in the γ lobe, we focused our analyses on the MBON dendrites in the compartments γ2 through γ5.

We first examined how ablation of individual MBONs that target their dendrites to specific compartments of the γ lobe would affect the targeting of MBON dendrites in the neighboring compartments. We quantified the compartment-specific targeting of MBON dendrites by measuring the distance from their lateral or medial edge of their dendritic field to the midline of the brain. We found that ablation of MBON-γ3 neurons led to dramatic expansion of the dendritic field of MBON-γ4 neurons into the γ3 compartment that was originally occupied by MBON-γ3 neuron dendrites as indicated by the increase in the distance from the lateral edge of the dendritic field of MBON-γ4 neurons to the midline of the brain, and sit next to axons (Fig. 1C, L). The dendritic field of MBON-γ4 neurons expanded all the way to the lateral edge of the axonal field of PPL1-γ2α'1 (simplified as PPL1-γ2 hereafter) neurons but did not further invade into the γ2 compartment (Fig. 1E). Meanwhile, the dendritic field of MBON-γ2 neurons also expanded slightly but significantly into the original γ3 compartment as indicated by the decrease in the distance from the medial edge of the axonal field to the midline (Fig. 1E, M). These results indicate that MBON-γ3 neurons may express a repulsive cue to repel MBON-γ4 dendrites and MBON-γ2 neuron axons either directly or indirectly and prevent

them from projecting into the γ3 compartment. Furthermore, either PPL1-γ2 or MBON-γ2 neurons may also express a repulsive molecule that could repel MBON-γ4 dendrites as the expanded MBON-γ4 dendrites did not invade into the γ2 compartment.

In addition to MBON-γ3 neurons, we found that genetic ablation of MBON-γ4 neurons also resulted in projection of some dendritic processes of MBON-γ3 neurons and MBON-γ5 neurons into the γ4 compartment (Fig. 1F-G, N-O), suggesting that MBON-γ4 neurons may also express a repulsive cue to repel dendrites of MBON-γ3 and MBON-γ5 neurons. However, we did not observe projection of MBON-γ3 neuron dendrites into the γ2 compartment or MBON- γ4 neuron dendrites into the γ5 compartment when MBON- γ2 neurons or MBON- γ5 neurons were ablated, respectively (Supplemental Fig. S2A-D), suggesting that MBON-γ2 neurons and MBON-γ5 may not express repulsive molecules to repel MBON dendrites from neighboring compartments.

Next, we investigated if ablation of DANs would affect the targeting of MBON dendrites. We ablated either individual type or a small subset of DAN neurons depending on the GAL4 lines used. We found that ablation of PPL1-γ2 neurons led to dramatic expansion of the dendritic field of MBON-γ3 neurons into the γ2 compartment and displacement of the dendrites of MBON-γ2 neurons from the γ2 compartment, but no obvious overlap between them (Fig. 1H, P). These phenotypes suggest that PPL1-γ2 neurons may express a repulsive cue to prevent MBON-γ3 dendrites from projecting into the γ2 compartment. The displacement of MBON-γ2 neuron dendrites from the γ2

compartment further supports that MBON-γ3 neurons may express a repulsive cue to repel MBON-γ2 dendrites.

Additionally, we found that ablation of PAM-γ3, PAM-γ4, and PAM-γ5 DAN neurons all together using *R58E02-GAL4* led to dramatic expansion of the dendritic field of MBON-γ4 and MBON-γ5 neurons and invasion into each other's territories, resulting nearly complete overlap between MBON-γ4 dendrites and MBON-γ5 dendrites and loss of the gap between MBON-γ5 dendrites and MBON-γ3 dendrites (Fig. 1I-I", Q-R, Fig. 2G-H'). These results suggest that these DAN neurons, particularly PAM-γ4 and PAM-γ5 neurons, also regulate compartment-specific targeting of dendrites of MBON-γ4 and MBON-γ5 neurons. They may do so either by providing repulsive cues to repel dendrites of MBONs from neighboring compartments or by providing attractive cues to restrict the projection of the dendrites of their partner MBON neurons to the same compartment. To distinguish these two possibilities, we then ablated PAM-γ3 and PAM-γ4 neurons only by simultaneously expressing GAL80 to inhibit the expression of *UAS-hid*^{ala5} in PAM-γ5 neurons. We found that ablation of PAM-γ3 and PAM-γ4 neurons alone led to projection of only MBON-γ5 neuron dendrites into the γ4 compartment, but not the projection of MBON-γ4 neuron dendrites into the γ5 compartment (Fig. 1J-J", Q-R). By specifically labelling MBON-γ3 neuron and MBON-γ4 neurons while ablating PAM-γ3 and PAM-γ4 neurons, we observed that MBON-γ3 dendrites also expanded into the γ4 compartment, overlapping with MBON-γ4 dendrites (Fig. 1K-K", S). However, ablation of PAM-γ3 neurons alone did not affect the targeting of the dendrites of MBON-γ3 or MBON-γ4

neurons (Supplemental Fig. 2E-F). These results suggest that PAM-γ5 neurons likely express a repulsive cue to prevent the projection of MBON-γ4 dendrites into the γ5 compartment and PAM-γ4 neurons may express a different repulsive molecule to repel the dendrites of both MBON-γ3 and MBON-γ5 neurons, whereas PAM-γ3 neurons may not have an obvious role in regulating the projection of the dendrites of MBON-γ3 and MBON-γ4 neurons.

Together, these genetic ablation results demonstrate that compartment-specific targeting of MBON dendrites is at least in part regulated by repulsive interactions between neighboring compartments. The repulsion can be mediated by either MBONs or DANs. However, since MBON dendrites still projected to the MB γ axonal lobe when their dendritic fields expanded due to the genetic ablation, the MB γ neurons likely also provide attractive cues to guide the projection of MBON dendrites to the γ lobe.

PPL1-γ2 and PAM-γ5 neurons express Slit that repels MBON dendrites and DAN axons from the γ3 and γ4 compartments

What molecules could mediate the repulsion between neighboring compartments? Interestingly, previous studies have shown that a GAL4 enhancer trap line, *slit*-GAL4^{NP2755} (Tanaka et al. 2008), in which the GAL4 transgene is integrated in the first intron of *slit*, is also expressed in PPL1-γ2 and PAM-γ5 neurons (Fig. 2A-A”). In addition, the *R32F01-GAL4* line that is driven by an enhancer fragment *R32F01* from *slit* is also expressed in PPL1-γ2 (Fig. 2B-B”) (Pfeiffer et al. 2008; Jenett et al. 2012), suggesting

that Slit, a classic repulsive molecule (Rothberg et al. 1988), could be expressed in PPL1-γ2 and PAM-γ5 neurons to repel MBON dendrites and/or DAN axons from neighboring compartments. To confirm the expression of Slit in these neurons, we performed immunofluorescent staining using the published Slit antibody (Rothberg et al. 1990). Consistently, we detected Slit protein in the soma of PPL1-γ2 neurons by immunostaining and the staining signal was abolished by RNAi knockdown (Supplemental Fig. S3B-B', D-D'). However, we were not able to determine if Slit is expressed in the γ2 or γ5 compartment by immunostaining due to ubiquitous Slit staining signals in the entire MB axonal lobes and the dendritic area of the MB, the calyx, as reported previously (Supplemental Fig. 3A-A', B-B') (Oliva et al. 2016). We did not observe obvious reduction of the staining signal in the MB when *elav-GAL4* drove the expression of *UAS-Slit RNAi* pan-neuronally even though MB axonal lobes were mis-targeted as previously reported (Supplemental Fig. S3E-F) (Oliva et al. 2016). Furthermore, expression of *UAS-Slit RNAi* driven by MB-specific *GAL4-OK107* led to neither reduction of Slit staining in the MB axonal lobes nor obvious targeting defects of MB axonal lobes (Supplemental Fig. S3G-H), suggesting that the targeting defects of MB axons resulting from the pan-neuronal expression of *UAS-slit RNAi* is likely non-cell autonomous. Finally, expression of *UAS-slit* driven by MB γ neuron-specific *GAL4*^{NP21} could not rescue the targeting defects of MB γ lobe in *slit* mutants (Supplemental Fig. S3I-K). Therefore, we conclude that the staining signal in the MB is non-specific, which is consistent with the lack of expression of *slit-GAL4*^{NP2755} and *R32F01-GAL4* in MB neurons.

To functionally validate if PPL1-γ2 and PAM-γ5 neurons indeed express Slit to repel MBON dendrites and DAN axons from the γ3 and γ4 compartments, we examined how targeting of MBON dendrites and DAN axons in the γ3 and γ4 compartment would be affected when Slit is knocked down in PPL1-γ2 or PAM-γ5 neurons or mutated. Our results showed that knockdown of Slit in PPL1-γ2 neurons led to projection of MBON-γ3 neuron dendrites into the γ2 compartment and extensive overlap with PPL1-γ2 neuron axons, which remained in the γ2 compartment. Furthermore, the entire dendritic field of MBON-γ3 neuron also shifted laterally as indicated by the increase in the distance from the medial edge of the dendritic field of MBON-γ3 neurons to the midline of the brain (Fig. 2B-C", F). However, the lateral shift of the dendritic field of MBON-γ3 neurons cannot fully account for the projection of MBON-γ3 neuron dendrites into the γ2 compartment because the increase in the distance from the lateral edge of the dendritic field of MBON-γ3 neurons to the midline is far greater than the increase in the distance from the medial edge to the midline (Fig. 2F). Similarly, we found that knockdown of Slit in PAM-γ5 neurons led to projection of MBON-γ4 neuron dendrites into the γ5 compartment and overlap with PAM-γ5 axons. Furthermore, the entire dendritic field of MBON-γ4 neurons also slightly shifted medially as indicated by the decrease in the distance from the lateral edge of the dendritic field to the midline (Fig. 2D-E", G).

Consistent with Slit knockdown, we observed that in $slit^{2}/slit^{Dui}$ trans-heterozyous mutant brains, MBON-γ3 neuron dendrites also projected into the γ2 compartment and overlapped with MBON-γ2 dendrites and PPL1-γ2 axons (Supplemental Fig. S4A-A", C-

C”). In some cases, the MBON-γ2 neurons dendrites were also displaced from the original γ2 compartment like when PPL1-γ2 neurons were ablated. Similarly, MBON-γ4 neuron dendrites also overlapped with MBON-γ5 neurons dendrites (Supplemental Fig. S4E-E”). The overlap of MBON-γ3 neuron dendrites with PPL1-γ2 neuron axons could be largely rescued by expressing *UAS-slit* in PPL1-γ2 neurons (Supplemental Fig. 4D-D”). However, expression of *UAS-slit* in MBON-γ2 neurons did not restore the sharp boundary between MBON-γ3 neurons dendrites and MBON-γ2 neurons dendrites (Supplemental Fig. S4B-B”), further confirming that PPL1-γ2 neurons express Slit to repel MBON-γ3 neuron dendrites but not MBON-γ2 neurons.

Expression of Robo receptors in MBONs and DANs

Slit functions as a repulsive molecule by binding to its Robo receptors. In *Drosophila*, there are three Robo receptors, Robo1, Robo2, and Robo3 (Kidd et al. 1999; Simpson et al. 2000b). To investigate how Slit repels MBON dendrites in the γ3 and γ4 compartments, we first wanted to determine which neurons express which Robo receptors. We examined the expression of Robo1 and Robo3 by immunostaining using their existing antibodies, and Robo2 using a Cherry protein trap line Robo2^{Cherry} (Sasse and Klambt 2016). Since the γ lobe undergo remodeling during early pupal stages (Technau and Heisenberg 1982; Lee et al. 1999) and the projection patterns of MBON dendrites observed in adult brains might be established after remodeling of the γ lobe, we examined their expression at about 2-3 days after puparium formation (APF), when the γ lobe just finishes remodeling and the expression of Robo receptors might be

higher than that at adult stages. We found that all these Robo receptors are expressed in both γ3 and γ4 compartments (Fig. 3A1-A1', B1-B1', C1-C1'). The expression levels of Robo1 are comparable in these two compartments, where Robo2 and Robo3 have higher expression levels in the γ4 compartment than in the γ3 compartment.

To determine the sources of the expression of these Robo receptors in the γ3 or γ4 compartments, we then examined if the expression of these Robo receptors in the γ3 or γ4 compartments would be reduced when *UAS-RNAi* transgenes against Robo1, Robo2, or Robo3 were expressed in MBON-γ3, MBON-γ4, PAM-γ3, or PAM-γ4 neurons. We found that expression of *UAS-robo1 RNAi* in MBON-γ3 but not in PAM-γ3 neurons nearly abolished the expression of Robo1 expression in the γ3 compartment, whereas expression of *UAS-robo1 RNAi* in MBON-γ4 or PAM-γ4 both led to 40-50% reduction of Robo1 expression in the γ4 compartment (Fig. 3A2-A5', D), suggesting that Robo1 is expressed in MBON-γ3, MBON-γ4, and PAM-γ4 neurons but probably not in PAM-γ3 neurons.

For Robo2, we found that Robo2^{cherry} expression is abolished in the γ3 or γ4 compartment when *UAS-robo2 RNAi* was expressed in MBON-γ3 or PAM-γ4 neurons, respectively (Fig. 3B1-B4', E). Consistently, we observed the expression of Robo2^{cherry} in the soma of MBON-γ3 or PAM-γ4 neurons was also abolished when *UAS-robo2 RNAi* was expressed in these neurons (insets in Fig. 3B1-B4'). However, no Robo2^{cherry} expression was detected in the soma of PAM-γ3 or MBON-γ4 neurons (Fig. 3B5-B6').

These data indicate that Robo2 is expressed in MBON-γ3 and PAM-γ4 neurons but not in PAM-γ3 or MBON-γ4 neurons.

For Robo3, we found that Robo3 expression in the γ3 was reduced by about 50% when *UAS-robo3* RNAi was expressed in either PAM-γ3 or MBON-γ3 neurons (Fig. 3C1-C3', F). In the γ4 compartment, Robo3 expression was abolished only when *UAS-robo3 RNAi* was expressed in PAM-γ4 but not MBON-γ4 neurons (Fig. 3C4-C5', F). indicating that Robo3 is expressed in PAM-γ3, MBON-γ3, and PAM-γ4 neurons but not MBON-γ4 neurons. In support of this conclusion, two GAL4 transgenic lines, *R46A06-GAL4* and *R46F02-GAL4*, driven by enhancer fragments from *robo3*, have also been shown to be expressed in PAM-γ4 and MBON-γ3 neurons, respectively (Jenett et al. 2012).

Taken together, these expression data from the wild type and RNAi knockdown brains indicate that 1) MBON-γ3 and PAM-γ4 neurons express all three Robo receptors; 2) MBON-γ4 neurons express Robo1 alone; and 3) PAM-γ3 neurons express Robo3 alone (Fig. 3G).

Different Robo receptors mediate compartment-specific targeting of MBON dendrites and DAN axons in the γ3 and γ4 compartments

Next we investigated if these Robo receptors are indeed involved in regulating the compartment-specific targeting of MBON dendrites and/or DAN axons the γ3 and γ4 compartments by examining how knockdown of these Robo receptors would affect the

targeting of their dendrites or axons in these two compartments in adult brains. Since different Robo receptors could function redundantly (Rajagopalan et al. 2000a; Rajagopalan et al. 2000b; Simpson et al. 2000a; Simpson et al. 2000b; Tayler et al. 2004), we knocked down different Robo receptors individually or simultaneously. We first examined how knockdown of Robo receptors would affect the targeting of MBON-γ3 neuron dendrites. Our results showed that knockdown of Robo1 alone in MBON-γ3 neurons led to projection of their dendrites into the γ2 compartment. Similar phenotypes were observed with two independent *UAS-robo1 RNAi* lines (Bloomington *Drosophila* Stock Center (BDSC) lines #35768 and #39027) (Fig. 4A-C, S), suggesting that Robo1 is required to restrict the growth of MBON-γ3 neuron dendrites within the γ3 compartment. However, the line #35768 gave stronger phenotypes than the line #39027. When Robo1 was knocked down with the line #39027, MBON-γ3 dendrites invading the γ2 compartment were less dense (as measured by the relative GFP intensities) than those in the γ3 compartment and MBON-γ2 neuron dendrites remained in the γ2 compartment, whereas with the line #35768, the dendrites of MBON-γ3 invading the γ2 compartment were almost equally dense as those in the γ3 compartment and MBON-γ2 neuron dendrites were largely displaced from the γ2 compartment (Fig. 4B-C, T). In contrast, double knockdown of Robo2 and Robo3 in MBON-γ3 neurons did not affect targeting of MBON-γ3 neuron dendrites (Fig. 4D, S). However, simultaneous knockdown of Robo2 or Robo3 enhanced the phenotypes resulting from Robo1 knockdown with the weaker line #39027. The dendrites of MBON-γ3 neurons invading the γ2 compartment became equally dense as in the γ3 compartment and the dendrites of MBON-γ2 neurons were also displaced from the γ2

compartment (Fig. 4E-F, S-T) as observed when Robo1 was knocked down with the stronger line #35768. These data suggest that Robo receptors are required to prevent the projection of MBON-γ3 neuron dendrites into the γ2 compartment. This is primarily mediated by Robo1, but Robo2 and Robo3 have partial redundant functions.

Like MBON-γ3 neurons, we found that knockdown of Robo1 led to projection of MBON-γ4 neuron dendrites into the γ5 compartment, overlapping with MBON-γ5 neuron dendrites (Fig. 4G-H', U). However, most dendrites of Robo1 knockdown MBON-γ4 neurons remained in the γ4 compartment and knockdown of Robo1 with the line #35768 did not give stronger phenotypes than the line #39027 (Fig. 4H-H', U-V). Further, consistent with no expression of Robo2 or Robo3 in MBON-γ4 neurons, double knockdown of Robo2 and Robo3 did not affect the projection of MBON-γ4 dendrites (Fig. 4I), nor did they enhance the phenotypes resulting from Robo1 knockdown with the weaker line #39027 (Fig. 4J-J', U-V). The relative density of MBON-γ4 dendrites in the γ4 and γ5 compartments, as measured by the intensity of RFP expressed in MBON-γ4 neuron dendrites, did not change significantly when all three Robo receptors were simultaneously knocked down compared to Robo1 knockdown alone (Fig. 4H-H', J-J', V). These results suggest that Robo1 is also required to prevent MBON-γ4 neurons from projecting their dendrites into the γ5 compartment, but Robo2 and Robo3 are not. Similar projection of MBON-γ4 dendrites into the γ5 compartment resulting from Robo1 knockdown in MBON-γ4 neurons and Slit knockdown in PAM-γ5 neurons further confirm that PAM-γ5 neurons express Slit to repel MBON-γ4 neuron dendrites. The expression

of Robo1 in MBON-γ4 neurons also explains why the MBON-γ4 dendrites would not project into the γ2 compartment and overlap with PPL1-γ2 axons when MBON-γ3 neurons were ablated as Slit expressed in PPL1-γ2 could repel MBON-γ4 dendrites. However, given that most MBON-γ4 neuron dendrites remained in the γ4 compartment after Robo1 or Slit knockdown, it is likely that other repulsive mechanisms may also be involved in preventing the projection of MBON-γ4 neuron dendrites into the γ5 compartment.

In PAM-γ3 and PAM-γ4 neurons, we found that knockdown of Robo3 alone was sufficient to cause the projection of their axons into the γ2 and γ5 compartments, respectively, although most of their axons remained in the γ3 or γ4 compartment, respectively (Fig. 4K-L, Q-R', W-X). In PAM-γ4 neurons, the Robo3 knockdown phenotypes were further enhanced by simultaneous knockdown of Robo1 or/and Robo2 receptors although double knockdown of Robo1 and Robo2 had no obvious effects (Fig. 4M-P, X-Y). PAM-γ4 neuron axons occupied both the γ4 and γ5 compartments with similar densities when all three Robo receptors were knocked down simultaneously (Fig. 4P, Y). Therefore, Robo receptors are also required for restricting the projection of the axons of PAM-γ3 and PAM-γ4 neurons to their specific compartments. However, unlike MBON-γ3 and MBON-γ4 neurons that rely primarily on Robo1, PAM-γ3 and PAM-γ4 neurons primarily depend on Robo3 for the compartment-specific targeting of their

Taken together, the Robo knockdown phenotypes and the expression patterns of Robo receptors demonstrate that Robo receptors are required for restricting the projection of

dendrites of MBON-γ3 and MBON-γ4 neurons and axons of PAM-γ3 and PAM-γ4 neurons to their specific compartments. However, different neurons use different combination of Robo receptors for regulating the compartment-specific targeting of their dendrites or axons.

Slit-mediated repulsion is required only during early pupal stages for the establishment of the compartment-specific targeting of MBON-γ3 neuron dendrites but not maintenance

To further elucidate cellular mechanisms underlying the compartment-specific targeting of MBON dendrites, we then investigated when the Slit-mediated repulsion occurs during development by examining the projection of PPL1-γ2 axons and MBON-γ3 neuron dendrites at different developmental stages in wild type and Slit knockdown brains. Since the MB γ lobe undergoes remodeling during early pupal stages (Technau and Heisenberg 1982; Lee et al. 1999), we examined the targeting of MBON-γ3 dendrites and PPL1-γ2 axons before, during, and after the remodeling of the γ lobe. In the wild type 3rd instar larval brains, PPL1-γ2 neurons (also named DAN-d1 in larval brains) projected their axons from the lateral side of the base to the tip of the lateral appendix, a short axonal lobe projecting from the junction of the medial and vertical axonal lobes of the MB γ neurons, whereas the dendrites of MBON-γ3 neurons (also named MBON-h1 in larval brains) projected to the middle/shaft of the medial lobe of the MB γ neurons (Fig. 5A-A') (Pauls et al. 2010; Truman et al. 2023). By co-labeling PPL1-γ2 and MBON-γ3 neurons with different fluorescent colors, it is obvious that MBON-γ3

dendrites and PPL1-γ2 axons do not physically contact with each other like in the adult brain (Fig. 5A-A”). Therefore, there may not be contact-dependent repulsive interactions between PPL1-γ2 axons and MBON-γ3 dendrites at the larval stages.

From 0 hrs APF to 14 hours APF, when axons of larval γ neurons are being pruned, MBON-γ3 dendrites gradually came close to PPL1-γ2 axons (Fig. 5B-C). Meanwhile, the dendrites of MBON-γ3 neurons became less dense and had lots of short spikes like filopodia pointing to all different directions at the peripheral of the dendritic field, indicating that MBON-γ3 dendrites were undergoing reorganization/growth and actively exploring their environment but were not pruned like the γ axons. By 16-18 hrs APF when the γ lobe was completely pruned, MBON-γ3 dendrites were physically next to PPL1-γ2 axons (Fig. 5D-E), but they never crossed the boundary to overlap with PPL1-γ2 axons afterwards (Fig. 5F-G), indicating that after they physically contact with each other, Slit secreted from PPL1-γ2 neurons prevents MBON-γ3 dendrites from projecting further laterally. With the progress of development, the medial edge of the dendritic field of MBON-γ3 neurons also gradually shifted laterally and their dendritic field became narrower (Fig. 5B-G). By 30 hrs APF when the γ lobe had re-extended, MBON-γ3 dendrites and PPL1-γ2 axons had largely established their adult projection patterns (Fig. 5G).

Consistent with the observation that MBON-γ3 dendrites come to physically contact with PPL1-γ2 axons only at early pupal stages but not at larval stages, we found that when

Slit was knocked down in PPL1-γ2 neurons, MBON-γ3 neuron dendrites did not display obvious targeting defects or overlap with PPL1-γ2 axons from 3rd instar larval stage to 16 hrs APF (Fig. 5H-J). However, at 18 hrs APF, MBON-γ3 dendrites started to grow into the γ2 compartment and overlapped with PPL1-γ2 axons (Fig. 5K). By 24-26 hrs APF, more extensive overlap between MBON-γ3 dendrites and PPL1-γ2 axons was observed (Fig. 5L-M). The projection of MBON-γ3 dendrites at larval and early pupal stages in the wild type and Slit knockdown brains demonstrate that repulsion of MBON-γ3 dendrites by Slit secreted from PPL1-γ2 neurons occurs only at early pupal stages but not larval stages.

Next, we asked whether Slit-mediated repulsion is continuously required to maintain the compartment-specific targeting of MBON-γ3 neuron dendrites after it is established at early pupal stages. To address this question, we ablated PPL1-γ2 neurons or knocked down Robo1 and Robo3 simultaneously in MBON-γ3 neurons after 4 days APF using *tub-GAL80^{ts}* (McGuire et al. 2003) to temporarily control the expression of *UAS-hid* and *UAS-rpr*, or *UAS-RNAi* transgenes and examined the projection of MBON-γ3 dendrites at 18 days after eclosion. Our results showed that ablation of PPL1-γ2 neurons or knockdown of Robo1 and Robo3 after 4 days APF no longer affected the compartment-specific targeting of MBON-γ3 neuron dendrites. MBON-γ3 neuron dendrites did not project into the γ2 compartment or overlap with PPL1-γ2 axons even at 18 days after eclosion (Fig. 5N-O). Therefore, Slit-mediated repulsion is only required during the establishment of the compartment-specific targeting of MBON-γ3 dendrites at early

pupal stages. Once the projection pattern is established, Slit-mediated repulsion is no longer needed to maintain the compartment-specific targeting of MBON-γ3 dendrites.

MBON-γ3 dendrites form ectopic synaptic contacts with PPL1-γ2 axons in the absence of Robo receptors

MBON-γ3 neurons normally form synaptic contacts with PAM-γ3 neurons but not PPL1-γ2 neurons. The projection of MBON-γ3 dendrites into the γ2 compartment resulting from knockdown of Slit or Robo receptors led us to ask if MBON-γ3 neurons could form ectopic synaptic contacts with PPL1-γ2 neurons in the absence of Slit/Robo-mediated repulsion. To answer this question, we employed the GRASP (GFP Reconstitution Across Synaptic Partners) approach (Feinberg et al. 2008) . By expressing CD4-spGFP1-10 in MBON-γ3 neurons and CD4-spGFP11 in PAM-γ3 neurons, we could detect reconstituted GFP signals that largely overlapped with the presynaptic marker Bruchpilot tagged with mCherry (Brp-mCherry) expressed in PAM-γ3 neurons (Fig. 6A-A_1”). In contrast, expressing CD4-spGFP1-10 in MBON-γ3 neurons and CD4-spGFP11 in PPL1-γ2 neurons in wild type brains did not give any reconstituted GFP signals, indicating that GRASP could specifically detect synaptic contacts. However, when all three Robo receptors were knocked down in MBON-γ3 neurons, expressing CD4-spGFP1-10 in MBON-γ3 neurons and CD4-spGFP11 in PPL1-γ2 neurons also gave reconstituted GFP signals in the area where MBON-γ3 dendrites overlapped with PPL1-γ2 axons. These reconstituted GFP signals largely overlapped with the presynaptic marker Brp-mCherry (Berger-Muller et al. 2013) expressed in the PPL1-γ2 neurons as

observed in the wild type brains (Fig. 6C-C_1”). Therefore, Slit/Robo-mediated repulsion not only ensure that the projection of MBON-γ3 neuron dendrites is restricted to the γ3 compartment, but also prevent the formation of ectopic synaptic contacts between MBON-γ3 neurons and PPL1-γ2 neurons.

Knockdown of Robo receptors in MBON-γ3 neurons impacts aversive learning but not memory processing

Given that PPL1-γ2 and PAM-γ3 neurons respond to different sensory stimuli (Claridge-Chang et al. 2009; Aso et al. 2010; Aso et al. 2012; Liu et al. 2012), formation of ectopic synaptic contacts between MBON-γ3 neurons and PPL1-γ2 neurons could potentially led to miscommunications between these neurons, impairment of associative conditioning, and aberrant behavioral outputs. Therefore, we performed preliminary assessment of potential functional consequences of the defects of compartment-specific targeting of MBON-γ3 dendrites. We tested electric shock-reinforced aversive memory at 3 min, 3 hr, and 24 hr, after aversive olfactory conditioning. Since knockdown of Robo1 receptors in MBON-γ3 neurons led to consistent and dramatic expansion of MBON-γ3 neuron dendrites into the γ2 compartment, we performed memory tests on flies with Robo1 knockdown in MBON-γ3 neurons. Before aversive olfactory conditioning, Robo1 knockdown flies showed similar avoidance to the odors (octanol and methylcyclohexanol) and electric shocks used for training as wild type control flies (Fig. 7D-F), indicating that olfactory acuity and shock reactivity were not affected by Robo1 knockdown in MBON-γ3 neurons. After conditioning, we found that Robo1

knockdown flies had significantly enhanced performance at 3 min after conditioning. The performance index was enhanced by nearly 30% in Robo1 knockdown flies compared to control flies (Fig. 7A). However, the short-term (3 hr) and long-term (24 hr) memory showed no significant difference between Robo1 knockdown and control flies (Fig. 7B-C). In both groups, the performance index was reduced to about 0.3 at 3 hrs and 0.1 at 24 hrs after conditioning. This suggests that Robo1 knockdown most likely impacts the learning process, without affecting later stages of memory processing, such as memory consolidation or retrieval.

DISCUSSION

Subcellular specificity is a common feature of neuronal connections. Previous studies proposed that subcellular specificity of synaptic contacts can be controlled by the localized expression of cell surface molecules at subcellular domains of target neurons and/or guidance molecules expressed in neighboring guidepost cells (Ango et al. 2004; Colon-Ramos et al. 2007; Ango et al. 2008; Fazzari et al. 2010; Anderson et al. 2017; Favuzzi et al. 2019; Sales et al. 2019; Sando et al. 2019). Using the MBONs and DANs as a model system, we demonstrate in this study that mutual repulsive interactions between neighboring compartments is critical for regulating the subcellular specificity of targeting of dendrites and axons. These mutual repulsive interactions can be axon-axon, axon-dendrite, or dendrite-dendrite. We identified Slit as a repulsive molecule that mediates such repulsions between a subset of the compartments in the γ lobe (Fig. 7G).

Mutual repulsive interactions between neighboring compartments restricts the growth of MBON dendrites and DAN axons to their specific compartments

Our results from genetic ablation demonstrate that targeting of MBON dendrites to their specific compartments in the MB axonal lobes involves repulsive interactions between neighboring compartments. We show that ablation of a subset of MBONs or DANs leads to expansion of MBON dendrites into neighboring compartments. The repulsion can be mediated either by MBONs or DANs. From our ablation results, at least PPL1-γ2, MBON-γ3, MBON-γ4, PAM-γ4, and PAM-γ5 neurons can all repel MBON dendrites from neighboring compartments. The repulsion can be axon-dendrite (e.g. between PPL1-γ2 neuron axons and MBON-γ3 neuron dendrites), axon-axon (e.g. between PPL1-γ2 neuron axons and PAM-γ3 neuron axons), or dendrite-dendrite (e.g. between MBON-γ4 neuron dendrites and MBON-γ3 neuron dendrites). Furthermore, repulsions between neighboring compartments are likely mutual. For example, between the γ2 and γ3 compartments, PPL1-γ2 neuron axons repel MBON-γ3 neuron dendrites, whereas MBON-γ3 neuron dendrites possibly repel MBON-γ2 neuron dendrites. Between the γ3 and γ4 compartments, MBON-γ3 neuron dendrites and MBON-γ4 neuron dendrites likely mutually repel each other.

Since MBONs and DANs still targeted their dendrites and axons to the MB axonal lobe when the repulsive mechanisms are disabled either by genetic ablation or RNAi knockdown of Slit/Robo, repulsive interactions between neighboring compartments are

likely only responsible for restricting the growth of MBON dendrites and DAN axons to their specific compartments, but not their targeting to the MB axonal lobes. Targeting of MBON dendrites and DAN axons to the γ lobe is likely guided by attractive molecules expressed in the MB axonal lobes and different MB axonal lobes may express different attractive cues. This attractive mechanism is also demonstrated by recent studies showing that in the absence of the α lobe, PPL1-α'2α2 neuron axons fail to be targeted their specific compartments although they can still be targeted diffusely to a region around their specific compartments (Lin et al. 2022), whereas disrupting the Dpr12-Dipδ-mediated attractive interaction between the MB γ lobe and PAM-γ4/5 axons leads to shortening of the γ lobe and failure of the targeting of PAM-γ4/5 axons to the γ4 and γ5 compartments (Bornstein et al. 2021). However, we do not think that such attractive interactions as mediated by Dpr12-Dipδ is critical for restricting the growth of DAN axons to their specific compartments as suggested previously (Bornstein et al. 2021) because PAM-γ4 axons could expand into the γ5 compartment when Robo receptors were knocked down. Therefore, compartment-specific targeting of MBON dendrites and DAN axons likely involves a combination of different mechanisms, including both repulsive and attractive interactions. Attractive molecules locally expressed in the MB axonal lobes (either from MB neurons or other neurons) may first guide the projection of MBON dendrites and/or DAN axons to a specific MB axonal lobe. Then the repulsive interactions between neighboring compartments restrict the growth of MBON dendrites and DAN axons to their specific compartment.

Slit-Robo mediated repulsion regulates compartment-specific targeting of MBON dendrites and DAN axons in the γ3 and γ4 compartments

In this study, we identified Slit as a repulsive molecule that mediates repulsion between neighboring compartments. We show that Slit is expressed in PPL1-γ2 and PAM-γ5 neurons to repel both MBON dendrites and DAN axons from the γ3 and γ4 compartments, respectively. Interestingly, different MBONs and DANs express different Robo receptors to mediate the repulsion by Slit. MBON-γ3 and PAM-γ4 neurons express all three different Robo receptors, but Robo1 is the one that plays the primary role in mediating the repulsion. Robo2 and Robo3 may just play supplemental roles in these neurons. In contrast, MBON-γ4 and PAM-γ3 neurons only express Robo1 and Robo3 alone, respectively, to mediate the repulsion of Slit. Why these neurons express different Robo receptors for mediating the repulsion of Slit is an interesting question to be addressed in the future. In *Drosophila* ventral nerve cord, expression of different combination of Robo receptor determines the strength of the response and the distance of longitudinal axons from the midline (Rajagopalan et al. 2000b; Simpson et al. 2000a). Midline axons express Robo1 alone and are closest to the midline, whereas lateral axons that express Robo1 and Robo2 or all three Robo receptors are further pushed away from the midline. Similarly, positioning of different types of heart cells relative to the midline in *Drosophila* also depends on the expression of different Robo receptors (Santiago-Martinez et al. 2006). Therefore, expression of different Robo receptors may determine the strength of the repulsion and different MBONs and DANs may require different strength of Slit-mediated repulsion to restrict the growth of their dendrites or

axons to their specific compartment. Co-expression of all three Robo receptors may confer the strongest repulsion, whereas expression of Robo3 or Robo1 alone confers weaker repulsion. For example, MBON-γ3 neuron dendrites may need stronger Slit-mediated repulsion than PAM-γ3 axons as more MBON-γ3 neuron dendrites will invade the γ2 compartment than PAM-γ3 axons in the absence of Slit-mediated repulsion. Most axons of PAM-γ3 neurons remain in the γ3 compartment. The reason could be that the attractive interactions of PAM-γ3 axons with MBON-γ3 neuron dendrites (see our companion paper) will also help restrict the growth of PAM-γ3 axons to the γ3 compartment and the Slit-mediated repulsion is just part of the mechanisms, thus PAM-γ3 neurons only need to express Robo3. Whereas MBON-γ3 neuron dendrites may rely solely on Slit-mediated the repulsion to avoid projecting into the γ2 compartment because MBON-γ3 neuron dendrites project to the γ3 compartment before the arrival PAM-γ3 axons (see our companion paper). Thus MBON-γ3 neurons express all three Robo receptors to have the strongest response to Slit. However, different Robo receptors may also have unique roles by activating different downstream signaling pathways as shown in midline crossing of commissural axons in *Drosophila* (Rajagopalan et al. 2000a; Simpson et al. 2000b; Spitzweck et al. 2010).

Further, our results demonstrate that Slit-mediated repulsions of MBON dendrites and DAN axons in the γ3 and γ4 compartments only occur in the early pupal stages but not larval stages. First, Slit-expressing PAM-γ5 neurons and Robo-expressing PAM-γ3 and PAM-γ4 neurons are all born post-embryonically and probably do not complete morphogenesis until early pupal stages (Lee et al. 2020; Truman et al. 2023). Second,

there is a big gap between MBON-γ3 neuron dendrites and PPL1-γ2 neuron axons in larval brains. Although Slit is a secreted molecule, it's diffusibility may be very limited and it may be anchored on the membrane of the cells that express Slit or on the immediate adjacent extracellular matrix as demonstrated previously (Wang et al. 1999; Nguyen-Ba-Charvet et al. 2001; Xiao et al. 2011; Wright et al. 2012). From our studies during early pupal stages, it is also obvious that extension of dendrites of MBON-γ3 neurons toward the future γ2 compartment won't stop until they reach the lateral edge of the axonal field of PPL1-γ2 neurons, suggesting that Slit-mediated repulsion of MBON-γ3 neuron dendrites is likely contact-dependent. Therefore, with a gap between MBON-γ3 neuron dendrites and PPL1-γ2 neuron axons, Slit expressed in PPL1-γ2 neurons won't repel MBON-γ3 dendrites in larval brains, which is supported by our results that knockdown of Slit in PPL1-γ2 neurons does not affect the targeting of MBON-γ3 dendrites at larval stages. It is possible that Slit expressed in PPL1-γ2 neurons may repel other MBON dendrites or MB input neuron (MBIN) axons targeted to the lower vertical lobe (LVL) compartment next to the lateral appendix (LA) compartment where axons of PPL1-γ2 neurons reside. Interestingly, Slit-mediated repulsion seems only required during the establishment of the projection of the MBON dendrites but not maintenance. Our results show that ablation of PPL1-γ2 neurons or knockdown of Robo receptors in MBON-γ3 neurons after 4 days APF no longer affects the projection of MBON-γ3 neuron dendrites. It is possible that after establishing their projection patterns, the MBON dendrites and DAN axons may have formed synaptic contacts, which help stabilize their projection. It is also possible that these neurons no longer actively grow/extend their dendrites or axons after forming synaptic contacts. Therefore, Slit-

mediated repulsion may be only required for establishing their projection patterns but not maintenance.

Functional consequences of the defects of compartment-specific targeting of MBON-γ3 dendrites

Functional significance of the compartment-specific targeting of MBON dendrites and DAN axons has never been assessed previous because it was hard to design a way to perturb their compart-specific targeting without knowing the underlying mechanisms. In this study, we were able to perturb the compartment-specific targeting of MBON-γ3 dendrites without affecting their targeting to the γ lobe by knocking down Slit or Robo. Our results show that invasion of MBON-γ3 dendrites into the neighboring γ2 compartment could potentially lead to formation of ectopic synaptic contacts with neighboring PPL1-γ2 axons and alteration of the performance of olfactory-associative learning. Thus, MBON dendrites have the capability to form synaptic contacts with DANs in other compartments, but compartment-specific targeting of MBON dendrites and DAN axons ensures the specificity of synaptic contacts between MBON dendrites and their partner DAN axons and proper learning and memory formation. The learning and memory phenotype observed in flies with Robo1 knockdown in MBON-γ3 might be explained by the ectopic synaptic connections form between MBON-γ3 dendrites and PPL1-γ2 axons. It is well established that MBON-γ3 neurons are GABAergic neurons, and its artificial optogenetic activation leads to attraction behavior (Aso et al. 2014a; Aso et al. 2014b). Similarly, optogenetic activation of MBON-γ2 also leads to attraction (Aso

et al. 2014b). Furthermore, aversive olfactory conditioning results in robust synaptic depression of MBON-γ2 in response to the trained odor, reducing attraction and leading to aversive behavior (Berry et al. 2018). This learning-induced neuroplasticity is modulated by PPL1-γ2. It is possible that the ectopic synaptic connections formed between the invading MBON-γ3 dendrites and PPL1-γ2 axons may allow PPL1-γ2, which conveys unconditioned information, to induce synaptic depression in MBON-γ3 during aversive learning, resulting in even more reduced attraction and thus enhancing short-term memory performance. Although knocking down Robo1 in MBON-γ3 might also result in reduced synaptic connections between PPL1-γ2 and its partner MBON-γ2 , this would not explain the observed memory phenotype, as it would likely lead to reduced learning. However, a caveat to this discussion is that we did not examine how the genetic manipulations in MBONs affect the targeting of their axons, which could provide feedback signals to DANs.

MATERIALS AND METHODS

Fly husbandry and strains

For genetic ablation of MBONs or DANs, *UAS-hid*^{ala5} (Bergmann et al. 2002) (a gift from F. Pignoni) or *UAS-hid* together with *UAS-reaper (rpr)* (Zhou et al. 1997) were expressed using cell type-specific GAL4 drivers. *LexAop-GAL80* (Pfeiffer et al. 2010) (Bloomington Drosophila Stock Center [BDSC] #32217) driven by *R48H11-LexA* (BDSC #52745) was used in combination with *R58E02-GAL4* (BDSC #41347) to restrict the

expression *UAS-hid*^{ala5} to only PAM-γ3-4 neurons. *UAS-mCD8-GFP* (BDSC #31289), *UAS-myr-GFP* (BDSC #32196), *UAS-mCD8-RFP* (BDSC #32219), *UAS-myr-tdTomato* (BDSC #32221), and *LexAop-rCD2-RFP* (BDSC #58755) were used to label neurons of interest. *UAS-rCD2-RFP*; *UAS-CD4-spGFP1-10* (BDSC #67093) and *LexAop-CD4-spGFP11* (BDSC #93018) (Gordon and Scott 2009) were used for GRASP analyses. *LexAop-brp.s.mCherry* (a gift from W.B. Grueber) (Berger-Muller et al. 2013) was used for labeling presynaptic boutons. *UAS-slit RNAi* (BDSC #31468), *sli*^{Dui} (Karpen and Spradling 1992) (BDSC #9284) and *sli*^{2} (Nambu et al. 1990) (BDSC #3266) were used for Slit loss-of-function analyses. *UAS-sli*.D (BDSC stock #67688) was used for rescuing *sli*^{2}*/sli*^{Dui} mutant phenotypes. Robo2^{Cherry} (gifts from C. Klambt) (Sasse and Klambt 2016) were used for examining the endogenous expression patterns of Robo2. *UAS-robo1 RNAi* (BDSC stocks #35768 and #39027), *UAS-robo2 RNAi* (BDSC stock #34589), and *UAS-robo3 RNAi* (BDSC stock #9287) were used for knocking down Robo receptors. For the genetic ablation and RNAi knockdown, animals were raised at 29°C to enhance the expression of UAS-transgenes. For genetical ablation of PPL1-γ2 neurons or knockdown of Robo receptors specifically after 4 days APF, *tub-GAL80*^{ts} (McGuire et al. 2003) was used in combination with cell type-specific GAL4 lines and animals were maintained at 18°C until they were shifted to 29°C at 4 days APF. GAL4 and LexA lines used for driving the expression of UAS/LexAop-transgenes are listed in the Table 1 below.

Table 1. GAL4/LexA lines used for different types of neurons

Neurons	GAL4/LexA lines	stock #

MBON-γ2α'1	split MBON-γ2α'1-GAL4	BDSC 68249
	R25D01-LexA	BDSC 49122
MBON-γ3	R94B10-GAL4	BDSC 41325
	split MBON-γ3-GAL4	BDSC 68287
MBON-γ4	R18H09-GAL4	BDSC 48830
	R53C03-GAL4	BDSC 38870
	R76B09-GAL4 split MBON-γ4-GAL4	BDSC 46962 BDSC 68309
MBON-γ5	R27G01-GAL4	BDSC 49233
	split MBON-γ5-GAL4	BDSC 68272
PPL1-γ2	R32F01-GAL4	BDSC 49359
	split PPL1-γ2-GAL4	BDSC 68279 and 68290
	R73F07-LexA	BDSC 52743
PAM-γ3	R48B03-GAL4	BDSC 50346
	split PAM-γ3-GAL4	BDSC 68251
	R48B03-LexA	BDSC 54214
PAM-γ4	R46A06-GAL4	BDSC 50250
PAM-γ5	R48H11-GAL4	BDSC 50396
	split PAM-γ5-GAL4	BDSC 48316
	R48H11-LexA	BDSC 52745

PAM-γ3-5	R58E02-GAL4	BDSC 41347
PAM-γ4-5	R48B04-GAL4	BDSC 50347
PAM-γ5 and PPL1-γ2	Gal4-NP2755	DGRC 113037
pan-neuronal	Elav-GAL4	BDSC 458
all MB neurons	Gal4-OK107	BDSC 854
MB γ neurons	Gal4-NP21	DGRC 103496

Construction of plasmids and generation of transgenic lines

For constructing *R27G01-mCD8-GFP*, *R94B10-mCD8-GFP*, and *R93D10-mCD8-GFP MBON-G1* plasmids, the corresponding enhancer fragments, R27G01, R94B10, and R93D10, flanked by restriction sites BglII and KpnI, were amplified by PCR from genomic DNA and cloned first into pJet2.1 vector. The enhancer fragments R27G01 and R94B10 were then cut from pJet2.1 vector with BglII and KpnI or NotI and NheI and two copies of each were incorporated into the pAPIC-PHsIH-3xmCD8::GFP vector (Han et al. 2011) between BglII and KpnI and between NotI and NheI, respectively, to replace the original *ppk* enhancer fragment. The R93D10 fragment was cut from pJet2.1 vector with NotI and NheI and only one copy of the fragment was incorporated into the pAPIC-PHsIH-3xmCD8::GFP vector using the same restrictions sites. The resulting constructs allow these enhancer fragments to drive the expression of three copies of mCD8::GFP.

The *R53C03-CD4-tdTomato* expression vector was constructed using the gateway technology. The R53C03 enhancer fragment amplified from genomic DNA by PCR with

the incorporation of the attB1 sequence at the 5'-end and the attB2 sequence at the 3'-end. The enhancer fragment was then cloned into the donor vector pDONR 211 (Invitrogen, Waltham, MA) at the attP1/attP2 sites through BP reactions. The resulting entry clone was then used to transit the enhancer fragment through LR reactions to the destination vector pDEST-HemmarR (Han et al. 2011), which allows the enhancer fragment to drive the expression of CD4-tdTomato.

Primers used to amplify the enhancer fragments were designed based on the sequences available from the Janelia FlyLight website (https://flweb.janelia.org/cgi-bin/flew.cgi) (Pfeiffer et al. 2008) and are listed below. The sequences in capital indicate the BglII site in the forward primers and KpnI site in the reverse primers for the amplification of R27G01, R94B10, and R93D10, and attB1 in the forward primer and attB2 in the reverse primer for the amplification of R53C03.

For amplification of R27G01 (2091 bps in length):

Forward: 5'-gacAGATCTggttggcgcagatagaacaacacga-3'

Reverse: 5'-gacGGTACCcttttctccagcgatgacgtcacca-3'

For amplification of R94B10 (1280 bps in length):

Forward: 5'-gacAGATCTaataaaagtcgcatggcggtggtga-3'

Reverse: 5'-gacGGTACCgtgtcgtaaagtcgaggtaattgcc-3'

For amplification of R93D10 (2930 bps in length):

Forward: 5'-gacAGATCTcccttgctttcttctcccacaatac-3'

Reverse: 5'-gacGGTACCcacgcccgaaatgaacggatcgaat-3'

For amplification of R53C03 (2651 bps in length):

Forward: 5'-GGGGACAAGTTTGTACAAAAAAGCAGGCTgctgctcggtctaatgatactggtc-3'

Reverse: 5'-GGGGACCACTTTGTACAAGAAAGCTGGGTctccaggataatggccgctatgaca-3'

The constructs were injected into *w*^{1118} *Drosophila* embryos by the Rainbow Transgenic Flies, Inc. (Camarillo, California). A standard P-element transposon protocol was used for the generation of the transformants.

Fluorescent immunostaining and Confocal microscopy imaging

Drosophila larval or adult brains were dissected and immunostained as previously described (Lee et al. 1999). Primary antibodies used include chicken anti-GFP (catalog #GFP-1020, Aves Labs, Tigard, Oregon; 1:500–1000), rabbit anti-DsRed (catalog #632496, Takara Bio USA, Inc., Mountain View, CA; 1:250), Chicken anti-spGFP1-10 (Abcam catalog # 13970, 1:1000), mouse anti-reconstituted spGFP1-10/spGFP11 (Sigma catalog# C6539, 1:100), mouse anti-Slit monoclonal antibody (1:15,catalog #C555.6D, RRID:AB_528470, Developmental Studies Hybridoma Bank [DSHB]) (Jhaveri et al. 2004), mouse anti-Robo1 monoclonal antibody (catalog #13C9, DSHB, 1:25) (Kidd et al. 1998), mouse anti-Robo3 monoclonal antibody (Catalog #14C9, DSHB, 1:25) (Simpson et al. 2000a), mouse anti-Fas II monoclonal antibody (catalog #1D4, DSHB, 1:50). Secondary antibodies conjugated to Daylight 488 (1:100), Cy3 (1:500),

Rhodamine Red-X (1:500), Daylight 647 (1:500) or Cy5 (1:500) used for immunostaining are from Jackson ImmunoResearch (West Grove, PA). Images were collected using a Carl Zeiss LSM780 confocal microscopy and processed with Adobe Photoshop.

Quantifications and Statistical analyses

For quantifying the distance from the lateral or medial edges of the dendritic field of MBONs or axonal field of DANs to the midline of the brain, we measured the distance from the midpoint of the medial or lateral edges to the midline and we chose the focal slice in the middle of the z-stack for the measurement. For quantifying staining intensities of Robo receptors in the γ3 or γ4 compartment in wild type or RNAi knockdown brains, the staining intensity was measured with the histogram in photoshop. The value was then subtracted by the background from areas with no Robo signals and normalized by the signal intensity (subtracted by the same background) in neighboring γ4 or γ3 compartment (i.e. quantification of the staining intensity in the γ3 compartment uses the staining intensity in the γ4 compartment for normalization, and *vice versa*). Student's *t*-test was used for statistical analyses. Graphs were generated with Microsoft Excel.

Aversive Olfactory Conditioning

Groups of 60 flies were first acclimated for ~15 min in a fresh food vial to the environment of a behavioral room dimly lit with red light at 24°C and 65% humidity. They were then transferred into a training tube where they received 30 sec of air,

followed by 1 min of an odor paired with 12 pulses of 90V electric shock (CS+), 30 sec of air, 1 min of a second odor with no electric shock (CS-), and finally 30 sec of air. For conditioning odors, we bubbled fresh air through 3-octanol (OCT) and 4-methylcyclohexonal (MCH) at concentrations of 0.07% and 0.12% in mineral oil, respectively. To measure three minutes memory, we immediately loaded the flies into a T-maze where they were allowed 2 min to choose between an arm with the CS+ odor and an arm with the CS- odor. To test memory retention at 3 and 24 h, we returned the flies after conditioning back into a food vial, for testing at a later time point. For all experiments, two groups were trained and tested simultaneously. One group was trained with OCT as the conditioned stimulus paired with reinforcer (CS+) and MCH unpaired with reinforcer (CS-), while the other group was trained with MCH as CS+ and OCT as CS-. Each group (60 flies) tested provided a half performance index (half PI): Half PI = ((# flies in CS- arm) – (# flies in CS+ arm)) / (# flies in both arms). A final PI was calculated by averaging the two half PI's. Since the two groups were trained to opposite CS+/CS- odor pairs, this method balanced out naïve odor biases.

ACKNOWLEDGEMENTS

We thank Drs. C. Klambt, W.B. Grueber for fly lines; the Bloomington *Drosophila* Stock Center and the TRiP at Harvard Medical School (NIH/NIGMS R01-GM084947), and Vienna *Drosophila* Resource Center for providing RNAi transgenic fly stocks; the Developmental Studies Hybridoma Bank for antibodies; members of the Zhu, Pignoni, and Lin Labs for thoughtful discussion and comments; Rainbow Transgenic Flies Inc for generating transgenic flies, Neuroscience Microscopy Core at Upstate Medical

University for providing Zeiss LSM 780 confocal microscopy. This work was supported by the National Institute of Neurological Disorders and Stroke of the National Institutes of Health under Award Number R01NS085232 (S.Z.), R21NS109748 (S.Z.), and R01GM147917 (I.C.S.).

AUTHOR CONTRIBUTIONS

Conceptualization, X.D, I.C.S., and S.Z.; Methodology: X.D., I.C.S., and S.Z.; Investigation: X.D. and I.C.S.; Data analysis: X.D., I.C.S., and S.Z.; Writing- Original Draft, S.Z., and I.C.S. and Writing- Review & Editing- S.Z., I.C.S., and X.D.; Supervision, S.Z.; Funding, S.Z. and I.C.S.

DECLARE OF INTERESTS

The authors declare no competing interests.

REFERENCES:

Anderson GR, Maxeiner S, Sando R, Tsetsenis T, Malenka RC, Sudhof TC. 2017. Postsynaptic adhesion GPCR latrophilin-2 mediates target recognition in entorhinal-hippocampal synapse assembly. *J Cell Biol* **216**: 3831-3846.

Ango F, di Cristo G, Higashiyama H, Bennett V, Wu P, Huang ZJ. 2004. Ankyrin-based subcellular gradient of neurofascin, an immunoglobulin family protein, directs GABAergic innervation at purkinje axon initial segment. *Cell* **119**: 257-272.

Ango F, Wu C, Van der Want JJ, Wu P, Schachner M, Huang ZJ. 2008. Bergmann glia and the recognition molecule CHL1 organize GABAergic axons and direct innervation of Purkinje cell dendrites. *PLoS Biol* **6**: e103.

Aso Y, Hattori D, Yu Y, Johnston RM, Iyer NA, Ngo TT, Dionne H, Abbott LF, Axel R, Tanimoto H et al. 2014a. The neuronal architecture of the mushroom body provides a logic for associative learning. *Elife* **3**: e04577.

Aso Y, Herb A, Ogueta M, Siwanowicz I, Templier T, Friedrich AB, Ito K, Scholz H, Tanimoto H. 2012. Three dopamine pathways induce aversive odor memories with different stability. *PLoS Genet* **8**: e1002768.

Aso Y, Sitaraman D, Ichinose T, Kaun KR, Vogt K, Belliart-Guerin G, Placais PY, Robie AA, Yamagata N, Schnaitmann C et al. 2014b. Mushroom body output neurons encode valence and guide memory-based action selection in Drosophila. *Elife* **3**: e04580.

Aso Y, Siwanowicz I, Bracker L, Ito K, Kitamoto T, Tanimoto H. 2010. Specific dopaminergic neurons for the formation of labile aversive memory. *Curr Biol* **20**: 1445-1451.

Baude A, Bleasdale C, Dalezios Y, Somogyi P, Klausberger T. 2007. Immunoreactivity for the GABAA receptor alpha1 subunit, somatostatin and Connexin36 distinguishes axoaxonic, basket, and bistratified interneurons of the rat hippocampus. *Cereb Cortex* **17**: 2094-2107.

Berger-Muller S, Sugie A, Takahashi F, Tavosanis G, Hakeda-Suzuki S, Suzuki T. 2013. Assessing the role of cell-surface molecules in central synaptogenesis in the Drosophila visual system. *PLoS One* **8**: e83732.

Bergmann A, Tugentman M, Shilo BZ, Steller H. 2002. Regulation of cell number by MAPK-dependent control of apoptosis: a mechanism for trophic survival signaling. *Dev Cell* **2**: 159-170.

Berry JA, Phan A, Davis RL. 2018. Dopamine Neurons Mediate Learning and Forgetting through Bidirectional Modulation of a Memory Trace. *Cell Rep* **25**: 651-662 e655.

Bornstein B, Meltzer H, Adler R, Alyagor I, Berkun V, Cummings G, Reh F, Keren-Shaul H, David E, Riemensperger T et al. 2021. Transneuronal Dpr12/DIP-delta interactions facilitate compartmentalized dopaminergic innervation of Drosophila mushroom body axons. *EMBO J* **40**: e105763.

Claridge-Chang A, Roorda RD, Vrontou E, Sjulson L, Li H, Hirsh J, Miesenbock G. 2009. Writing memories with light-addressable reinforcement circuitry. *Cell* **139**: 405-415.

Cognigni P, Felsenberg J, Waddell S. 2018. Do the right thing: neural network mechanisms of memory formation, expression and update in Drosophila. *Curr Opin Neurobiol* **49**: 51-58.

Cohn R, Morantte I, Ruta V. 2015. Coordinated and Compartmentalized Neuromodulation Shapes Sensory Processing in Drosophila. *Cell* **163**: 1742-1755.

Colon-Ramos DA, Margeta MA, Shen K. 2007. Glia promote local synaptogenesis through UNC-6 (netrin) signaling in C. elegans. *Science* **318**: 103-106.

Favuzzi E, Deogracias R, Marques-Smith A, Maeso P, Jezequel J, Exposito-Alonso D, Balia M, Kroon T, Hinojosa AJ, E FM et al. 2019. Distinct molecular programs regulate synapse specificity in cortical inhibitory circuits. *Science* **363**: 413-417.

Fazzari P, Paternain AV, Valiente M, Pla R, Lujan R, Lloyd K, Lerma J, Marin O, Rico B. 2010. Control of cortical GABA circuitry development by Nrg1 and ErbB4 signalling. *Nature* **464**: 1376-1380.

Feinberg EH, Vanhoven MK, Bendesky A, Wang G, Fetter RD, Shen K, Bargmann CI. 2008. GFP Reconstitution Across Synaptic Partners (GRASP) defines cell contacts and synapses in living nervous systems. *Neuron* **57**: 353-363.

Galindo SE, Wood AJ, Cooney PC, Hammond LA, Grueber WB. 2023. Axon-axon interactions determine modality-specific wiring and subcellular synaptic specificity in a somatosensory circuit. *Development* **150**.

Gordon MD, Scott K. 2009. Motor control in a Drosophila taste circuit. *Neuron* **61**: 373-384.

Guven-Ozkan T, Davis RL. 2014. Functional neuroanatomy of Drosophila olfactory memory formation. *Learn Mem* **21**: 519-526.

Han C, Jan LY, Jan YN. 2011. Enhancer-driven membrane markers for analysis of nonautonomous mechanisms reveal neuron-glia interactions in Drosophila. *Proc Natl Acad Sci U S A* **108**: 9673-9678.

Jenett A, Rubin GM, Ngo TT, Shepherd D, Murphy C, Dionne H, Pfeiffer BD, Cavallaro A, Hall D, Jeter J et al. 2012. A GAL4-driver line resource for Drosophila neurobiology. *Cell Rep* **2**: 991-1001.

Jhaveri D, Saharan S, Sen A, Rodrigues V. 2004. Positioning sensory terminals in the olfactory lobe of Drosophila by Robo signaling. *Development* **131**: 1903-1912.

Karpen GH, Spradling AC. 1992. Analysis of subtelomeric heterochromatin in the Drosophila minichromosome Dp1187 by single P element insertional mutagenesis. *Genetics* **132**: 737-753.

Kawaguchi Y, Kubota Y. 1997. GABAergic cell subtypes and their synaptic connections in rat frontal cortex. *Cereb Cortex* **7**: 476-486.

Kidd T, Bland KS, Goodman CS. 1999. Slit is the midline repellent for the robo receptor in Drosophila. *Cell* **96**: 785-794.

Kidd T, Brose K, Mitchell KJ, Fetter RD, Tessier-Lavigne M, Goodman CS, Tear G. 1998. Roundabout controls axon crossing of the CNS midline and defines a novel subfamily of evolutionarily conserved guidance receptors. *Cell* **92**: 205-215.

Klausberger T, Magill PJ, Marton LF, Roberts JD, Cobden PM, Buzsaki G, Somogyi P. 2003. Brain-state- and cell-type-specific firing of hippocampal interneurons in vivo. *Nature* **421**: 844-848.

Lee T, Lee A, Luo L. 1999. Development of the Drosophila mushroom bodies: sequential generation of three distinct types of neurons from a neuroblast. *Development* **126**: 4065-4076.

Lee YJ, Yang CP, Miyares RL, Huang YF, He Y, Ren Q, Chen HM, Kawase T, Ito M, Otsuna H et al. 2020. Conservation and divergence of related neuronal lineages in the Drosophila central brain. *Elife* **9**.

Lin CH, Senapati B, Chen WJ, Bansal S, Lin S. 2022. Semaphorin 1a-mediated dendritic wiring of the Drosophila mushroom body extrinsic neurons. *Proc Natl Acad Sci U S A* **119**: e2111283119.

Liu C, Placais PY, Yamagata N, Pfeiffer BD, Aso Y, Friedrich AB, Siwanowicz I, Rubin GM, Preat T, Tanimoto H. 2012. A subset of dopamine neurons signals reward for odour memory in Drosophila. *Nature* **488**: 512-516.

Mao Z, Davis RL. 2009. Eight different types of dopaminergic neurons innervate the Drosophila mushroom body neuropil: anatomical and physiological heterogeneity. *Front Neural Circuits* **3**: 5.

McGuire SE, Le PT, Osborn AJ, Matsumoto K, Davis RL. 2003. Spatiotemporal rescue of memory dysfunction in Drosophila. *Science* **302**: 1765-1768.

Miles R, Toth K, Gulyas AI, Hajos N, Freund TF. 1996. Differences between somatic and dendritic inhibition in the hippocampus. *Neuron* **16**: 815-823.

Nambu JR, Franks RG, Hu S, Crews ST. 1990. The single-minded gene of Drosophila is required for the expression of genes important for the development of CNS midline cells. *Cell* **63**: 63-75.

Nguyen-Ba-Charvet KT, Brose K, Marillat V, Sotelo C, Tessier-Lavigne M, Chedotal A. 2001. Sensory axon response to substrate-bound Slit2 is modulated by laminin and cyclic GMP. *Mol Cell Neurosci* **17**: 1048-1058.

Oliva C, Soldano A, Mora N, De Geest N, Claeys A, Erfurth ML, Sierralta J, Ramaekers A, Dascenco D, Ejsmont RK et al. 2016. Regulation of Drosophila Brain Wiring by Neuropil Interactions via a Slit-Robo-RPTP Signaling Complex. *Dev Cell* **39**: 267-278.

Owald D, Felsenberg J, Talbot CB, Das G, Perisse E, Huetteroth W, Waddell S. 2015. Activity of defined mushroom body output neurons underlies learned olfactory behavior in Drosophila. *Neuron* **86**: 417-427.

Pauls D, Selcho M, Gendre N, Stocker RF, Thum AS. 2010. Drosophila larvae establish appetitive olfactory memories via mushroom body neurons of embryonic origin. *J Neurosci* **30**: 10655-10666.

Perisse E, Owald D, Barnstedt O, Talbot CB, Huetteroth W, Waddell S. 2016. Aversive Learning and Appetitive Motivation Toggle Feed-Forward Inhibition in the Drosophila Mushroom Body. *Neuron* **90**: 1086-1099.

Pfeiffer BD, Jenett A, Hammonds AS, Ngo TT, Misra S, Murphy C, Scully A, Carlson JW, Wan KH, Laverty TR et al. 2008. Tools for neuroanatomy and neurogenetics in Drosophila. *Proc Natl Acad Sci U S A* **105**: 9715-9720.

Pfeiffer BD, Ngo TT, Hibbard KL, Murphy C, Jenett A, Truman JW, Rubin GM. 2010. Refinement of tools for targeted gene expression in Drosophila. *Genetics* **186**: 735-755.

Pouille F, Scanziani M. 2001. Enforcement of temporal fidelity in pyramidal cells by somatic feed-forward inhibition. *Science* **293**: 1159-1163.

Rajagopalan S, Nicolas E, Vivancos V, Berger J, Dickson BJ. 2000a. Crossing the midline: roles and regulation of Robo receptors. *Neuron* **28**: 767-777.

Rajagopalan S, Vivancos V, Nicolas E, Dickson BJ. 2000b. Selecting a longitudinal pathway: Robo receptors specify the lateral position of axons in the Drosophila CNS. *Cell* **103**: 1033-1045.

Rothberg JM, Hartley DA, Walther Z, Artavanis-Tsakonas S. 1988. slit: an EGF-homologous locus of D. melanogaster involved in the development of the embryonic central nervous system. *Cell* **55**: 1047-1059.

Rothberg JM, Jacobs JR, Goodman CS, Artavanis-Tsakonas S. 1990. slit: an extracellular protein necessary for development of midline glia and commissural axon pathways contains both EGF and LRR domains. *Genes Dev* **4**: 2169-2187.

Sales EC, Heckman EL, Warren TL, Doe CQ. 2019. Regulation of subcellular dendritic synapse specificity by axon guidance cues. *Elife* **8**.

Sando R, Jiang X, Sudhof TC. 2019. Latrophilin GPCRs direct synapse specificity by coincident binding of FLRTs and teneurins. *Science* **363**.

Santiago-Martinez E, Soplop NH, Kramer SG. 2006. Lateral positioning at the dorsal midline: Slit and Roundabout receptors guide Drosophila heart cell migration. *Proc Natl Acad Sci U S A* **103**: 12441-12446.

Sasse S, Klambt C. 2016. Repulsive Epithelial Cues Direct Glial Migration along the Nerve. *Dev Cell* **39**: 696-707.

Schroll C, Riemensperger T, Bucher D, Ehmer J, Voller T, Erbguth K, Gerber B, Hendel T, Nagel G, Buchner E et al. 2006. Light-induced activation of distinct modulatory neurons triggers appetitive or aversive learning in Drosophila larvae. *Curr Biol* **16**: 1741-1747.

Schwaerzel M, Monastirioti M, Scholz H, Friggi-Grelin F, Birman S, Heisenberg M. 2003. Dopamine and octopamine differentiate between aversive and appetitive olfactory memories in Drosophila. *J Neurosci* **23**: 10495-10502.

Sejourne J, Placais PY, Aso Y, Siwanowicz I, Trannoy S, Thoma V, Tedjakumala SR, Rubin GM, Tchenio P, Ito K et al. 2011. Mushroom body efferent neurons responsible for aversive olfactory memory retrieval in Drosophila. *Nat Neurosci* **14**: 903-910.

Simpson JH, Bland KS, Fetter RD, Goodman CS. 2000a. Short-range and long-range guidance by Slit and its Robo receptors: a combinatorial code of Robo receptors controls lateral position. *Cell* **103**: 1019-1032.

Simpson JH, Kidd T, Bland KS, Goodman CS. 2000b. Short-range and long-range guidance by slit and its Robo receptors. Robo and Robo2 play distinct roles in midline guidance. *Neuron* **28**: 753-766.

Spitzweck B, Brankatschk M, Dickson BJ. 2010. Distinct protein domains and expression patterns confer divergent axon guidance functions for Drosophila Robo receptors. *Cell* **140**: 409-420.

Takemura SY, Aso Y, Hige T, Wong A, Lu Z, Xu CS, Rivlin PK, Hess H, Zhao T, Parag T et al. 2017. A connectome of a learning and memory center in the adult Drosophila brain. *Elife* **6**.

Tanaka NK, Tanimoto H, Ito K. 2008. Neuronal assemblies of the Drosophila mushroom body. *J Comp Neurol* **508**: 711-755.

Tayler TD, Robichaux MB, Garrity PA. 2004. Compartmentalization of visual centers in the Drosophila brain requires Slit and Robo proteins. *Development* **131**: 5935-5945.

Technau G, Heisenberg M. 1982. Neural reorganization during metamorphosis of the corpora pedunculata in Drosophila melanogaster. *Nature* **295**: 405-407.

Truman JW, Price J, Miyares RL, Lee T. 2023. Metamorphosis of memory circuits in Drosophila reveals a strategy for evolving a larval brain. *Elife* **12**.

Wang KH, Brose K, Arnott D, Kidd T, Goodman CS, Henzel W, Tessier-Lavigne M. 1999. Biochemical purification of a mammalian slit protein as a positive regulator of sensory axon elongation and branching. *Cell* **96**: 771-784.

Wang Y, Toledo-Rodriguez M, Gupta A, Wu C, Silberberg G, Luo J, Markram H. 2004. Anatomical, physiological and molecular properties of Martinotti cells in the somatosensory cortex of the juvenile rat. *J Physiol* **561**: 65-90.

Wright KM, Lyon KA, Leung H, Leahy DJ, Ma L, Ginty DD. 2012. Dystroglycan organizes axon guidance cue localization and axonal pathfinding. *Neuron* **76**: 931-944.

Xiao T, Staub W, Robles E, Gosse NJ, Cole GJ, Baier H. 2011. Assembly of lamina-specific neuronal connections by slit bound to type IV collagen. *Cell* **146**: 164-176.

Yamagata N, Ichinose T, Aso Y, Placais PY, Friedrich AB, Sima RJ, Preat T, Rubin GM, Tanimoto H. 2015. Distinct dopamine neurons mediate reward signals for short- and long-term memories. *Proc Natl Acad Sci U S A* **112**: 578-583.

Yogev S, Shen K. 2014. Cellular and molecular mechanisms of synaptic specificity. *Annu Rev Cell Dev Biol* **30**: 417-437.

Zhou L, Schnitzler A, Agapite J, Schwartz LM, Steller H, Nambu JR. 1997. Cooperative functions of the reaper and head involution defective genes in the programmed cell death of Drosophila central nervous system midline cells. *Proc Natl Acad Sci U S A* **94**: 5131-5136.

Deng_Fig 1

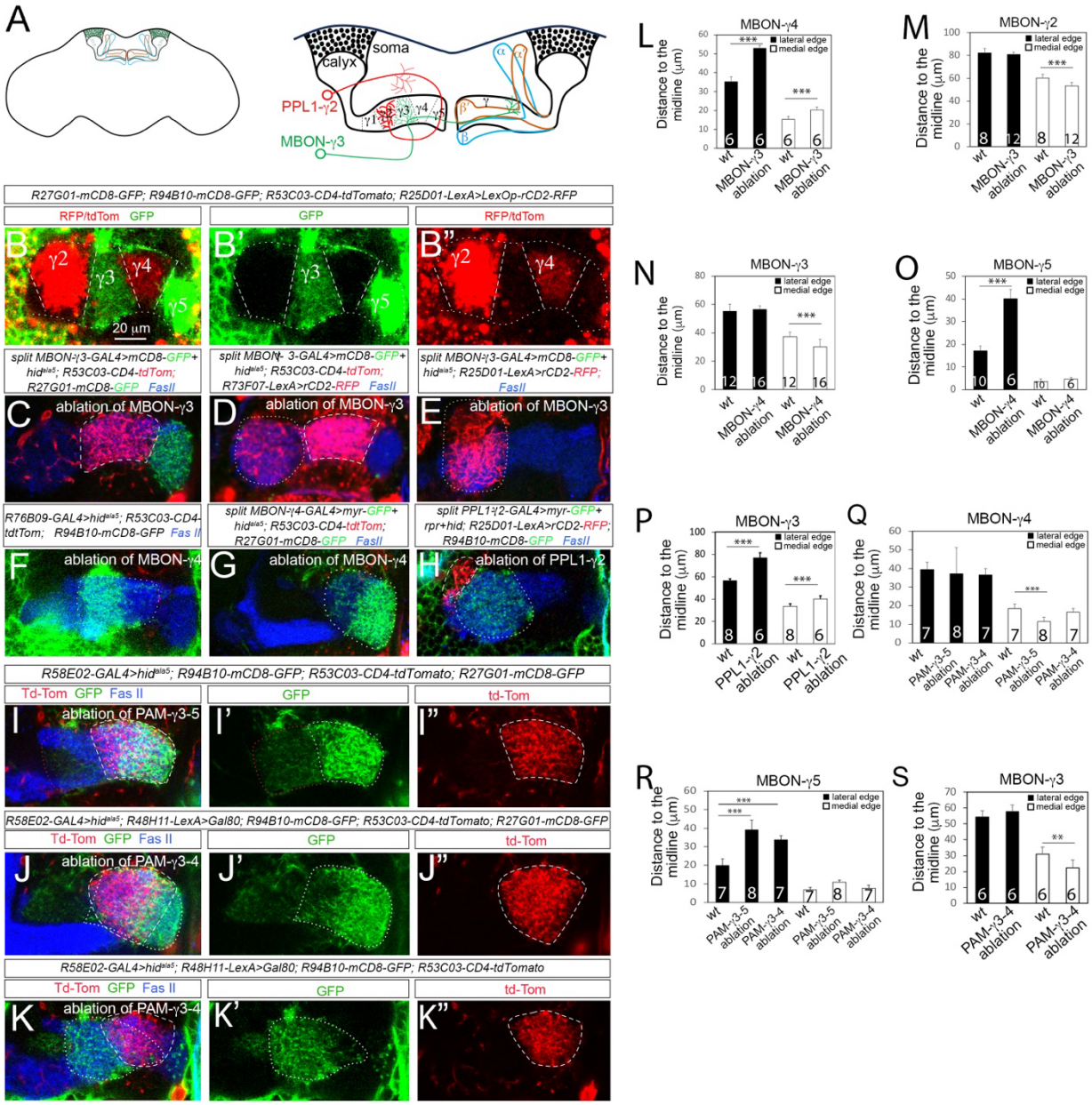
A
soma
calyx
PPL1-γ2
MBON-γ3
R27G01-mCD8-GFP; R94B10-mCD8-GFP; R53C03-CD4-tdTomato; R25D01-LexA>LexOp-rCD2-RFP
RFP/tdTom GFP
GFP
RFP/tdTom
20 μm
split MBON-γ3-GAL4>mCD8-GFP+ hid^bla5; R53C03-CD4-tdTom; R27G01-mCD8-GFP FasII
split MBON-γ3-GAL4>mCD8-GFP+ hid^bla5; R53C03-CD4-tdTom; R73F07-LexA>rCD2-RFP FasII
split MBON-γ3-GAL4>mCD8-GFP+ hid^bla5; R25D01-LexA>rCD2-RFP; FasII
ablation of MBON-γ3
R76B09-GAL4>hid^bla5; R53C03-CD4-tdTom; R94B10-mCD8-GFP Fas II
split MBON-γ4-GAL4>myr-GFP+ hid^bla5; R53C03-CD4-tdTom; R27G01-mCD8-GFP FasII
split PPL1γ2-GAL4>myr-GFP+ rpr+hid; R25D01-LexA>rCD2-RFP; R94B10-mCD8-GFP FasII
ablation of MBON-γ4
ablation of PPL1-γ2
R58E02-GAL4>hid^bla5; R94B10-mCD8-GFP; R53C03-CD4-tdTomato; R27G01-mCD8-GFP
Td-Tom GFP Fas II
td-Tom
ablation of PAM-γ3-5
R58E02-GAL4>hid^bla5; R48H11-LexA>Gal80; R94B10-mCD8-GFP; R53C03-CD4-tdTomato; R27G01-mCD8-GFP
ablation of PAM-γ3-4
R58E02-GAL4>hid^bla5; R48H11-LexA>Gal80; R94B10-mCD8-GFP; R53C03-CD4-tdTomato
MBON-γ4
MBON-γ2
MBON-γ3
MBON-γ5
Distance to the midline (μm)
lateral edge
medial edge
wt
MBON-γ3 ablation
MBON-γ4 ablation
PPL1-γ2 ablation
PAM-γ3-5 ablation
PAM-γ3-4 ablation

Fig. 1. Genetic ablation of MBONs or DANs leads to expansion of the dendritic fields of MBONs. (A) Schematic diagrams of the mushroom body (MB) in the fly brain (left) and an enlarged view of the MB that shows five compartments in the γ lobe and targeting of MBON-γ3 dendrites to the γ3 compartment and PPL1-γ2 axons to the γ2 compartment (right). (B-B") labeling of MBON dendrites in the γ2 through γ5 compartments with alternative fluorescent colors. Dotted lines outline the γ lobe and dashed lines demarcate the boundaries between neighboring compartments. (C-E) When MBON-γ3 neurons are ablated by the expression of Hid^{ala5}, MBON-γ4 dendrites (stronger RFP, dashed circles) expand into the γ3 compartment (C) and come next to PPL1-γ2 axons (weaker RFP, dotted circle) (D). MBON-γ2 neuron dendrites (dotted circle) also expanded slightly (E). (F-G) Ablation of MBON-γ4 neurons results in projection of MBON-γ3 dendrites (dotted circle) (F) and MBON-γ5 neuron dendrites (dashed circle) (G) dendrites into the γ4 compartment. (H) MBON-γ3 dendrites (dotted circle) project into the γ2 compartment when PPL1-γ2 neurons are ablated. MBON-γ2 dendrites (dashed circle) are largely displaced from the γ2 compartment and do not overlap with MBON-γ3 dendrites. (I-I") Ablation of PAM-γ3-5 neurons leads to expansion of MBON-γ4 dendrites (dashed circles) and MBON-γ5 dendrites (labeled with stronger GFP, white dotted circles) into each other's territories and extensive overlap between them. MBON-γ3 dendrites (labeled with weaker GFP, purple dotted circles) also project into the γ4 compartment and overlap with MBON-γ4 dendrites, leaving no gap between MBON-γ3 dendrites and MBON-γ5 dendrites. (J-K") Ablation of PAM-γ3-4 alone results in projection of MBON-γ5 dendrites (dotted circles) (J-J") and MBON-γ3 dendrites (dotted

circles) (K-K”) into the γ4 compartment and overlap with MBON-γ4 dendrites (dashed circles) without affecting the projection of MBON-γ4 dendrites. (L-S) Quantifications of the distance from the lateral (filled bars) or medial (open bars) edges to the midline of the brains of indicated MBONs in wild type brains or brains with ablation of indicated neurons. Numbers on individual bars represent the number of brain lobes examined. ***, $p<0.001$; **, $p<0.01$; compared to control groups; student *t*-test.

Deng_Fig 2

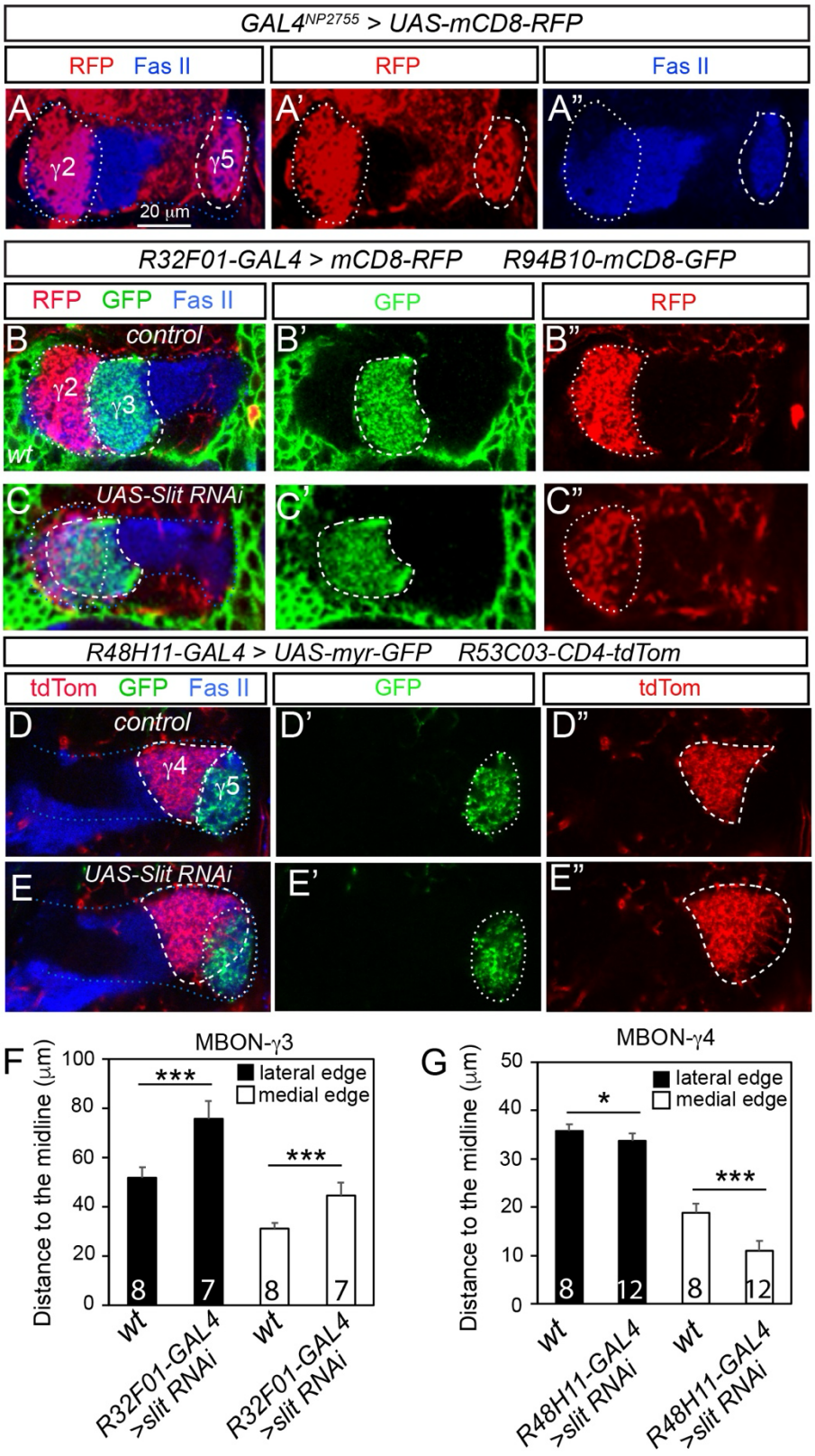
GAL4NP2755 > UAS-mCD8-RFP
RFP Fas II
RFP
Fas II
A
A'
A"
γ2
γ5
20 μm
R32F01-GAL4 > mCD8-RFP R94B10-mCD8-GFP
RFP GFP Fas II
GFP
RFP
B
control
γ2
γ3
wt
B'
B"
C
UAS-Slit RNAi
C'
C"
R48H11-GAL4 > UAS-myr-GFP R53C03-CD4-tdTom
tdTom GFP Fas II
GFP
tdTom
D
control
γ4
γ5
D'
D"
E
UAS-Slit RNAi
E'
E"
F
MBON-γ3
Distance to the midline (μm)
lateral edge
medial edge
***
***
8
7
8
7
wt
R32F01-GAL4 >slit RNAi
wt
R32F01-GAL4 >slit RNAi
G
MBON-γ4
Distance to the midline (μm)
lateral edge
medial edge
*
***
8
12
8
12
wt
R48H11-GAL4 >slit RNAi
wt
R48H11-GAL4 >slit RNAi

Fig. 2. Slit is expressed in PPL1-γ2 and PAM-γ5 neurons to repel MBON-γ3 and MBON-γ4 dendrites. (A-A") *GAL4*^{NP2755} is expressed in both PPL1-γ2 and PAM-γ5 neurons. Their axons in the γ2 and γ5 compartments are outlined with dotted and dashed circles, respectively. (B-B") GFP-labeled MBON-γ3 dendrites (dashed circles) and RFP-labeled PPL1-γ2 axons (dotted circles) occupy neighboring γ2 and γ3 compartment, respectively, without overlapping with each other in a wild type brain. (C-C") Knockdown of Slit in PPL1-γ2 neurons results in shifting and expansion of MBON-γ3 dendrites into the γ2 compartment, overlapping with PPL1-γ2 axons. (D-D") GFP-labeled PAM-γ5 axons (dotted circles) and RFP-labeled MBON-γ4 dendrites (dashed circles) occupy neighboring γ5 and γ4 compartment, respectively, without overlapping with each other in a wild type brain. (E-E") Slit Knockdown in PAM-γ5 neurons results in projection of MBON-γ4 dendrites into the γ5 compartment and overlap with PAM-γ5 axons. In all images, brains are counterstained with Fas II antibodies to labeled MB γ (outlined with blue dotted lines). (F-G) Quantifications of the distance from the lateral (filled bars) or medial (open bars) edges to the midline of the brains of MBON-γ3 (F) and MBON-γ4 (G) neurons in wild type or Slit knockdown brains. Numbers on individual bars represent the number of brain lobes examined. ***, $p<0.001$; *, $p<0.05$, compared to control groups; student *t*-test.

Deng_Fig 3

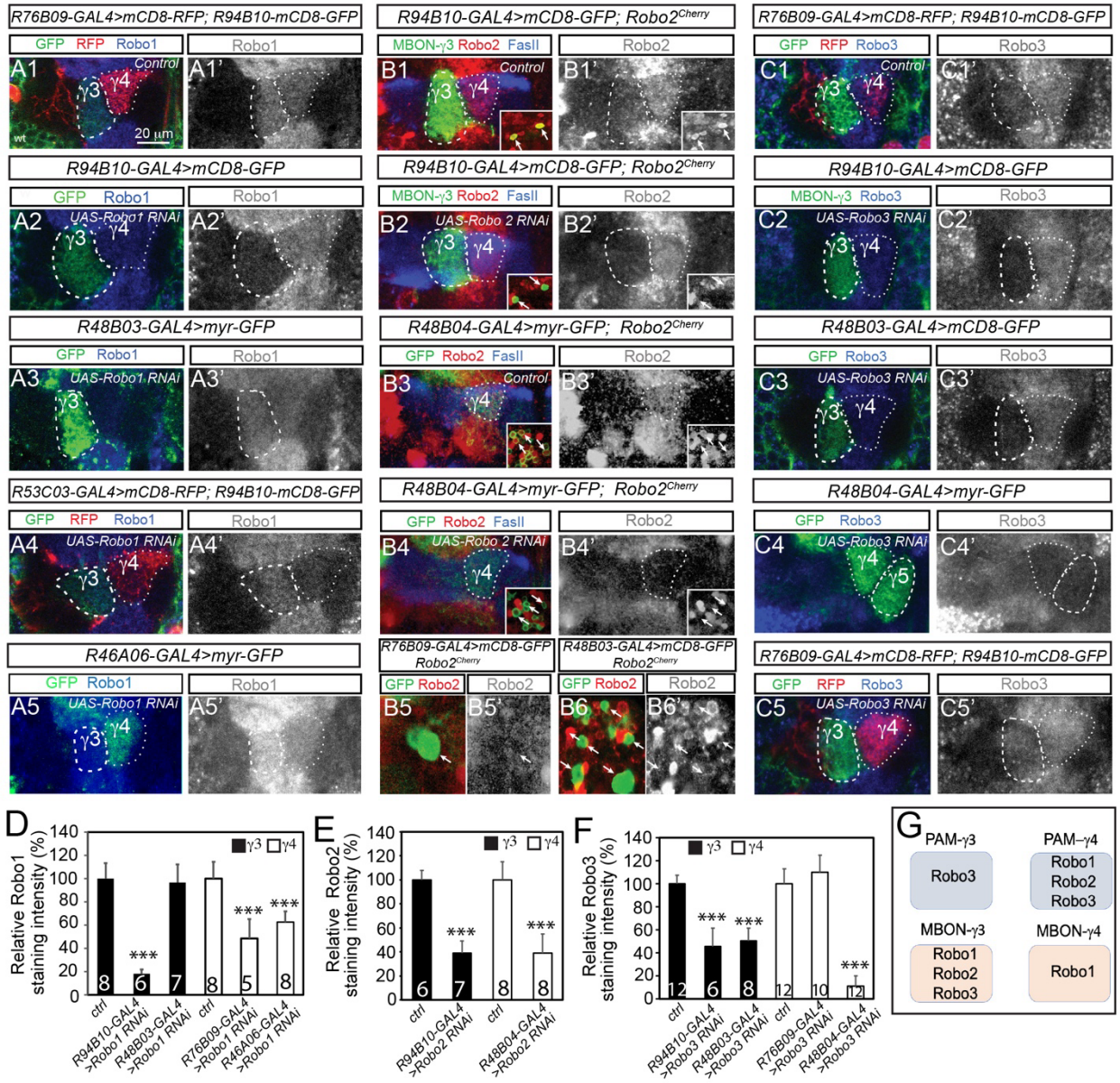
R76B09-GAL4>mCD8-RFP; R94B10-mCD8-GFP
GFP RFP Robo1
Robo1
A1
Control
γ3
γ4
wt
20 µm
A1'
R94B10-GAL4>mCD8-GFP; Robo2Cherry
MBON-γ3 Robo2 FasII
Robo2
B1
Control
B1'
R76B09-GAL4>mCD8-RFP; R94B10-mCD8-GFP
GFP RFP Robo3
Robo3
C1
Control
C1'
R94B10-GAL4>mCD8-GFP
GFP Robo1
Robo1
A2
UAS-Robo1 RNAi
A2'
R94B10-GAL4>mCD8-GFP; Robo2Cherry
MBON-γ3 Robo2 FasII
Robo2
B2
UAS-Robo 2 RNAi
B2'
R94B10-GAL4>mCD8-GFP
MBON-γ3 Robo3
Robo3
C2
UAS-Robo3 RNAi
C2'
R48B03-GAL4>myr-GFP
GFP Robo1
Robo1
A3
UAS-Robo1 RNAi
A3'
R48B04-GAL4>myr-GFP; Robo2Cherry
GFP Robo2 FasII
Robo2
B3
Control
B3'
R48B03-GAL4>mCD8-GFP
GFP Robo3
Robo3
C3
UAS-Robo3 RNAi
C3'
R53C03-GAL4>mCD8-RFP; R94B10-mCD8-GFP
GFP RFP Robo1
Robo1
A4
UAS-Robo1 RNAi
A4'
R48B04-GAL4>myr-GFP; Robo2Cherry
GFP Robo2 FasII
Robo2
B4
UAS-Robo 2 RNAi
B4'
R48B04-GAL4>myr-GFP
GFP Robo3
Robo3
C4
UAS-Robo3 RNAi
γ5
C4'
R46A06-GAL4>myr-GFP
GFP Robo1
Robo1
A5
UAS-Robo1 RNAi
A5'
R76B09-GAL4>mCD8-GFP Robo2Cherry
GFP Robo2
Robo2
B5
B5'
R48B03-GAL4>mCD8-GFP Robo2Cherry
GFP Robo2
Robo2
B6
B6'
R76B09-GAL4>mCD8-RFP; R94B10-mCD8-GFP
GFP RFP Robo3
Robo3
C5
UAS-Robo3 RNAi
C5'
D
Relative Robo1 staining intensity (%)
γ3 γ4
***
ctrl
R94B10-GAL4 >Robo1 RNAi
R48B03-GAL4 >Robo1 RNAi
R76B09-GAL4 >Robo1 RNAi
R46A06-GAL4 >Robo1 RNAi
E
Relative Robo2 staining intensity (%)
R94B10-GAL4 >Robo2 RNAi
R48B04-GAL4 >Robo2 RNAi
F
Relative Robo3 staining intensity (%)
R94B10-GAL4 >Robo3 RNAi
R48B03-GAL4 >Robo3 RNAi
R76B09-GAL4 >Robo3 RNAi
R48B04-GAL4 >Robo3 RNAi
G
PAM-γ3
Robo3
PAM–γ4
Robo1
Robo2
Robo3
MBON-γ3
Robo1
Robo2
Robo3
MBON-γ4
Robo1

Fig. 3. Expression of Robo receptors in MBONs and DANs. In all images, dashed circles outline the γ3 compartment except in (C4-C4') where they outline the γ5 compartment, and dotted circles outline the γ4 compartment. (A1-A1') Endogenous Robo1 proteins are expressed in the γ3 and γ4 compartments at similar levels in a wild type brain. Dendrites of MBON-γ3 and MBON-γ4 neurons are labeled with GFP and RFP to indicate the locations of γ3 and γ4 compartments, respectively. (A2-A3') Expression of Robo1 in the γ3 compartment was abolished by the expression of *UAS-Robo1 RNAi* in MBON-γ3 neurons using the line BDSC #39027 (A2-A2') but not in PAM-γ3 neurons using the line BDSC #35768 (A3-A3'). Both MBON-γ3 neurons (A2) and PAM-γ3 (A3) neurons are labeled with GFP. (A4-A5') Expression of *UAS-Robo1 RNAi* (BDSC #35768) in MBON-γ4 (A4-A4') or PAM-γ4 (A5-A5') neurons both leads to a significant reduction in the expression of Robo1 in the γ4 compartment. MBON-γ4 dendrites (A4) and PAM-γ4 axons (A5) are labeled with RFP and GFP, respectively, and outlined with dotted circles. MBON-γ3 neurons are labeled with GFP in (A4). (B1-B2') Robo2^{Cherry} expression is detected in the γ3 compartment and the soma of MBON-γ3 neurons in a wild type brain (B1-B1') but is dramatically reduced after expression of *UAS-Robo2 RNAi* in MBON-γ3 neurons (B2-B2'). Arrows in insets point to the soma of MBON-γ3 neurons. (B3-B4') Robo2^{Cherry} expression is detected in the γ4 compartment and the soma of PAM-γ4 neurons in a wild type brain (B3-B3') but is nearly abolished by the expression of *UAS-Robo2 RNAi* in PAM-γ4 neurons (B4-B4'). Arrows in insets point to the soma of PAM-γ4 neurons. (B5-B6') Robo2^{Cherry} expression is not detected in the soma (arrows) of MBON-γ3 (B5-B5') or PAM-γ3 (B6-B6') neurons. (C1-C1') Expression

of endogenous Robo3 is detected in both γ3 and γ4 compartments. Dendrites of MBON-γ3 and MBON-γ4 neurons are labeled with GFP and RFP, respectively. (C2-C3') Expression of *UAS-Robo3 RNAi* in MBON-γ3 neurons (C2-C2') or PAM-γ3 neurons (C3-C3') both leads to a significant reduction in the expression of Robo3 in the γ3 compartment. MBON-γ3 dendrites (C2) or PAM-γ3 axons (C3) are both labeled with GFP. (C4-C5') Expression of *UAS-Robo3 RNAi* in PAM-γ4-5 neurons (GFP) (C4-C4') but not MBON-γ4 neurons (RFP) (C5-C5') abolishes the expression of Robo3 in the γ4 compartment. MBON-γ3 neurons are labeled with GFP in (C5). (D-F) Quantifications of relative staining intensities of Robo1 (D), Robo2^{Cherry} (E), and Robo3 (F) in the γ3 and γ4 compartments in the brains with indicated genotypes. Numbers on individual bars represent the number of brain lobes examined. ***, $p<0.001$, compared to control groups; student *t*-test. (G) A diagram summarizing the expression of Robo1, Robo2, and Robo3 in of PAM-γ3 and PAM-γ4 axons and of MBON-γ3 and MBON-γ4 dendrites.

Deng_Fig 4

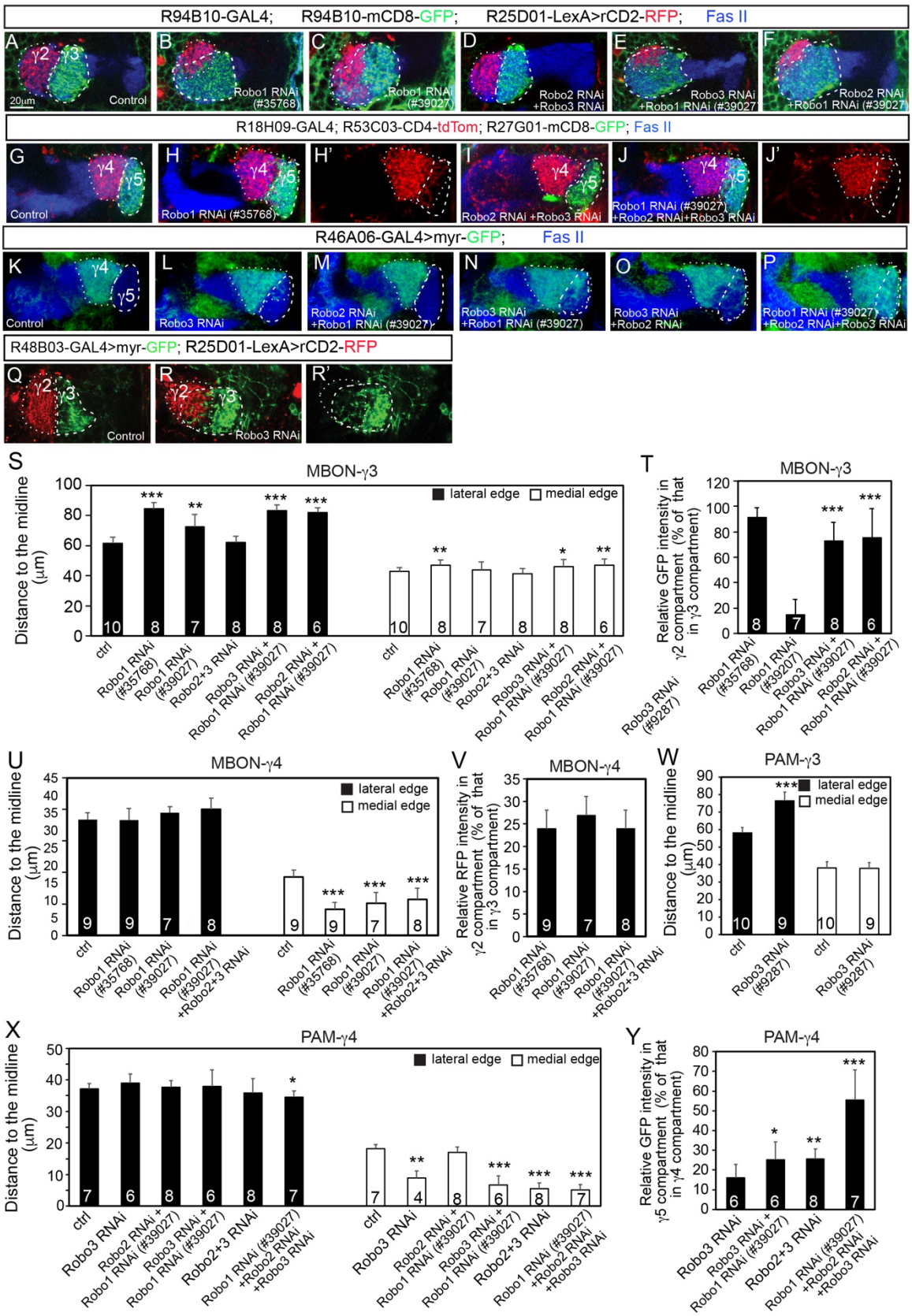
R94B10-GAL4; R94B10-mCD8-GFP; R25D01-LexA>rCD2-RFP; Fas II
A γ2 γ3 20μm Control
B Robo1 RNAi (#35768)
C Robo1 RNAi (#39027)
D Robo2 RNAi +Robo3 RNAi
E Robo3 RNAi +Robo1 RNAi (#39027)
F Robo2 RNAi +Robo1 RNAi (#39027)
R18H09-GAL4; R53C03-CD4-tdTom; R27G01-mCD8-GFP; Fas II
G γ4 γ5 Control
H γ4 γ5 Robo1 RNAi (#35768)
H'
I γ4 γ5 Robo2 RNAi +Robo3 RNAi
J γ4 γ5 Robo1 RNAi (#39027) +Robo2 RNAi+Robo3 RNAi
J'
R46A06-GAL4>myr-GFP; Fas II
K γ4 γ5 Control
L Robo3 RNAi
M Robo2 RNAi +Robo1 RNAi (#39027)
N Robo3 RNAi +Robo1 RNAi (#39027)
O Robo3 RNAi +Robo2 RNAi
P Robo1 RNAi (#39027) +Robo2 RNAi+Robo3 RNAi
R48B03-GAL4>myr-GFP; R25D01-LexA>rCD2-RFP
Q γ2 γ3 Control
R γ2 γ3 Robo3 RNAi
R'
S MBON-γ3
Distance to the midline (μm)
lateral edge
medial edge
ctrl
Robo1 RNAi (#35768)
Robo1 RNAi (#39027)
Robo2+3 RNAi
Robo3 RNAi + Robo1 RNAi (#39027)
Robo2 RNAi + Robo1 RNAi (#39027)
T MBON-γ3
Relative GFP intensity in γ2 compartment (% of that in γ3 compartment)
Robo3 RNAi (#9287)
U MBON-γ4
V MBON-γ4
Relative RFP intensity in γ2 compartment (% of that in γ3 compartment)
Robo1 RNAi (#39027) +Robo2+3 RNAi
W PAM-γ3
X PAM-γ4
Robo3 RNAi
Robo2 RNAi + Robo1 RNAi (#39027)
Robo1 RNAi (#39027) +Robo2 RNAi +Robo3 RNAi
Y PAM-γ4
Relative GFP intensity in γ5 compartment (% of that in γ4 compartment)

Fig. 4. Different Robo receptors are required to prevent the projection of MBON-γ3 and MBON-γ4 dendrites and of PAM-γ3 and PAM-γ4 axons into neighboring compartments.

(A-F) Projection of MBON-γ3 dendrites (GFP, dashed circle) and MBON-γ2 dendrites (RFP, dotted circle) in a wild type brain (A) or in brains with Robo1 knockdown alone with two independent *UAS-Robo1 RNAi* lines (B-C), double knockdown of Robo2 and Robo3 (D), Robo1 and Robo3 (E), or Robo1 and Robo2 (F) in MBON-γ3 neurons.

(G-J') Projection of dendrites of wild type (G), Robo 1 knockdown (H-H'), Robo2 and Robo3 double knockdown (I), and Robo1, Robo2, and Robo3 triple knockdown (J-J') MBON-γ4 neurons. MBON-γ4 dendrites are labeled with RFP (dotted circles). MBON-γ5 dendrites are labeled with GFP (dashed circles) to mark the γ5 compartment.

(K-P) Projection of PAM-γ4 axons (GFP, dotted circles) in a wild type brain (K), or brains with Robo3 knockdown alone (L), double knockdown of Robo1 and Robo2 (M), Robo1 and Robo3 (N), Robo2 and Robo3 (O), or triple knockdown of Robo1, Robo2, and Robo3 (P) in PAM-γ4 neurons. The γ5 compartment is outlined with dashed circles.

(Q-R') Projection of axons (GFP, dashed circles) of wild type (Q) and Robo3 knockdown (R-R') PAM-γ3 neurons. MBON-γ2 dendrites are labeled with RFP (dotted circles) to mark the γ2 compartment.

(S, U, W, X) Quantifications of the distance from the lateral or medial edge of the dendritic/axonal field of indicated neurons with knockdown of different Robo receptors to the midline in the brains. Numbers on individual bars represent the number of brain lobes examined. ***, $p<0.001$; **, $p<0.01$; *, $p<0.05$, compared to control groups; student *t*-test.

(T, V, Y) Quantifications of relative GFP intensities of indicated neurons with knockdown of different Robo receptors in their respective compartments. Numbers on individual bars represent the number of brain lobes examined. ***, $p<0.001$; **, $p<0.01$; *, $p<0.05$, compared to control groups; student *t*-test.

Deng_Fig 5

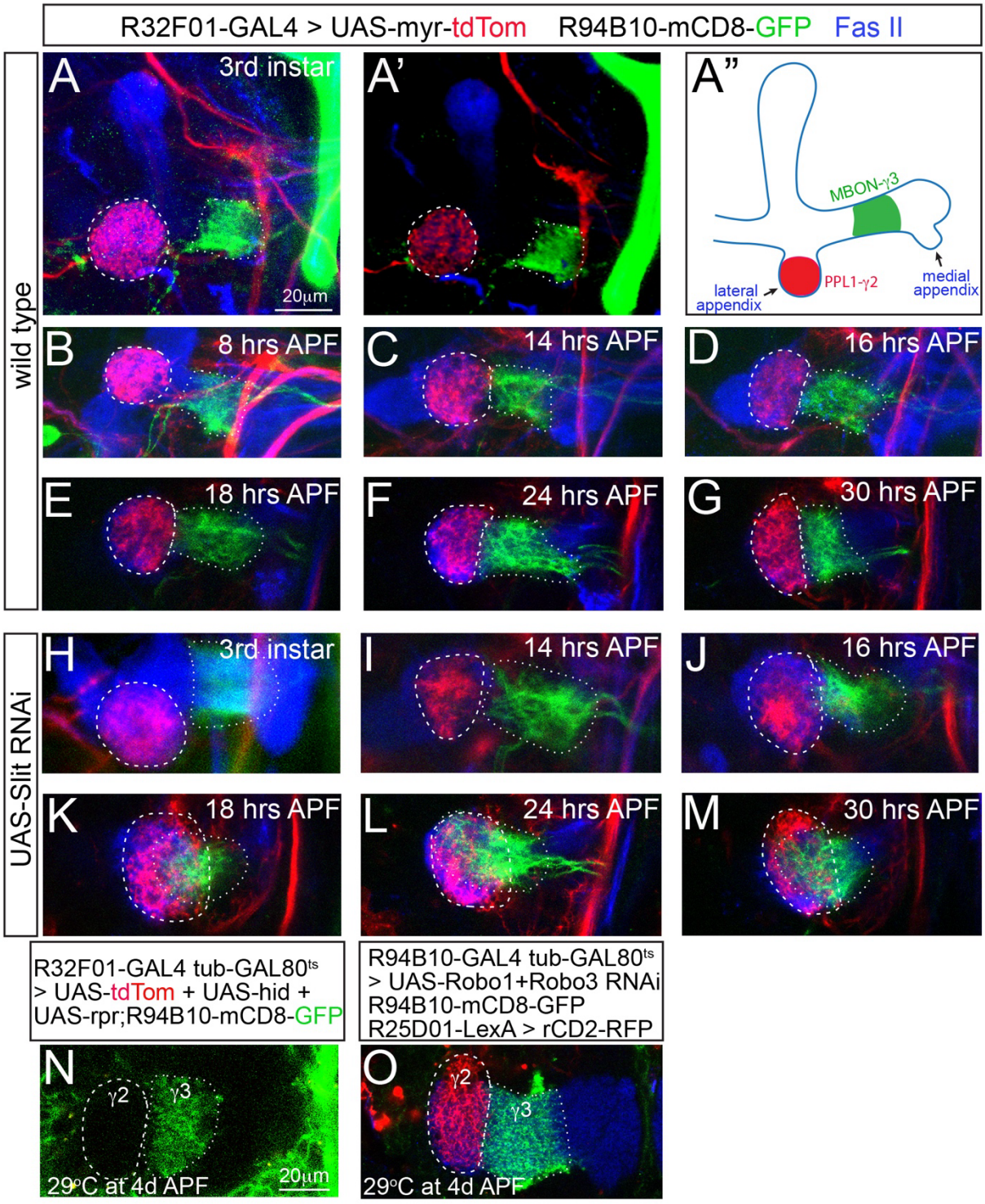
R32F01-GAL4 > UAS-myr-tdTom R94B10-mCD8-GFP Fas II
wild type
A
3rd instar
20µm
A'
A"
MBON-γ3
PPL1-γ2
lateral appendix
medial appendix
B
8 hrs APF
C
14 hrs APF
D
16 hrs APF
E
18 hrs APF
F
24 hrs APF
G
30 hrs APF
UAS-Slit RNAi
H
3rd instar
I
14 hrs APF
J
16 hrs APF
K
18 hrs APF
L
24 hrs APF
M
30 hrs APF
R32F01-GAL4 tub-GAL80ts > UAS-tdTom + UAS-hid + UAS-rpr;R94B10-mCD8-GFP
R94B10-GAL4 tub-GAL80ts > UAS-Robo1+Robo3 RNAi R94B10-mCD8-GFP R25D01-LexA > rCD2-RFP
N
γ2
γ3
29°C at 4d APF
20µm
O
γ2
γ3
29°C at 4d APF

Fig. 5. Projection of MBON-γ3 dendrites and PPL1-γ2 axons at different stages of development. In all images, MBON-γ3 dendrites are labeled with GFP and outlined with dotted circles. PPL1-γ2 axons are labeled with RFP and outlined with dashed circles. Brains are counterstained with anti-Fas II antibodies to mark MB axonal lobes. (A-G) Projection of PPL1-γ2 axons and MBON-γ3 dendrites during the 3rd instar larval stage (A-A") and early pupal stages (B-G) in wild type animals. (A') is a 3D-rendering of the same image shown in (A) to better show the gap between PPL1-γ2 axons and MBON-γ3 dendrites. (A") A schematic drawing of the localizations of PPL1-γ2 axons and MBON-γ3 dendrites in larval MB axonal lobes. (H-M) Projection of MBON-γ3 dendrites at the 3rd instar larval stage (H) and early pupal stages (I-M) when Slit is knocked down in PPL1-γ2 neurons. (N-O) MBON-γ3 dendrites (GFP, dotted circles) do not project into the γ2 compartment (dashed circles) and overlap with PPL1-γ2 axons (RFP) when PPL1-γ2 neurons are ablated after 4 days APF or when Robo1 and Robo3 are knocked down after 4 days APF.

Deng_Fig 6

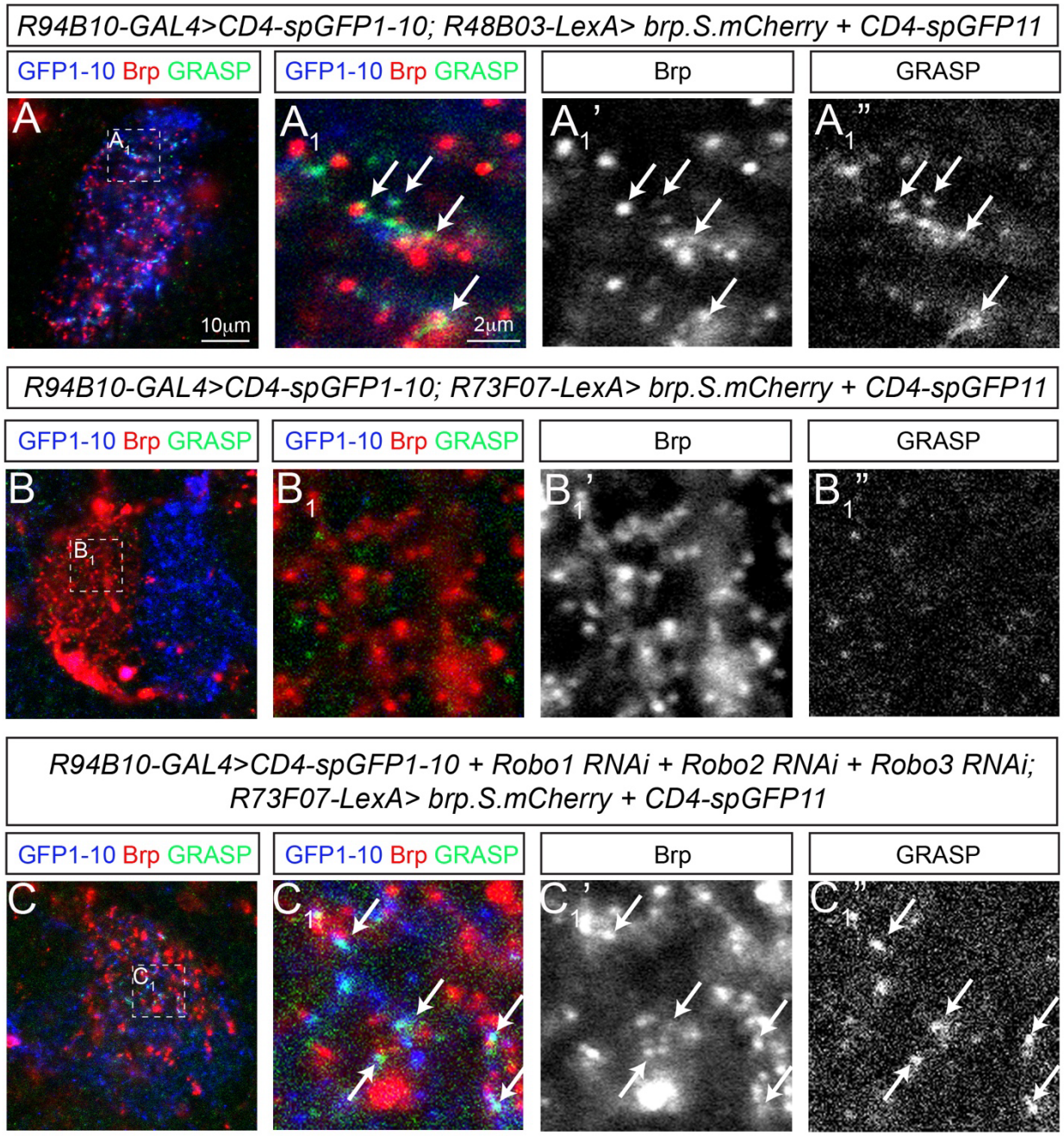
R94B10-GAL4>CD4-spGFP1-10; R48B03-LexA> brp.S.mCherry + CD4-spGFP11
GFP1-10 Brp GRASP
GFP1-10 Brp GRASP
Brp
GRASP
A
A1
10μm
2μm
A1'
A1"
R94B10-GAL4>CD4-spGFP1-10; R73F07-LexA> brp.S.mCherry + CD4-spGFP11
GFP1-10 Brp GRASP
GFP1-10 Brp GRASP
Brp
GRASP
B
B1
B1'
B1"
R94B10-GAL4>CD4-spGFP1-10 + Robo1 RNAi + Robo2 RNAi + Robo3 RNAi;
R73F07-LexA> brp.S.mCherry + CD4-spGFP11
GFP1-10 Brp GRASP
GFP1-10 Brp GRASP
Brp
GRASP
C
C1
C1'
C1"

Fig. 6. Mis-targeted MBON-γ3 dendrites potentially form ectopic synaptic contacts with PPL1-γ2 axons. (A-A_1”) GRASP signals are detected between MBON-γ3 dendrites and PAM-γ3 axons in a wild type brain. (A_1-A_1”) is an enlarged view of the area highlighted with a dashed square in (A). GRASP puncta (arrows) largely overlap with or are in close proximity of the presynaptic marker Brp-mCherry expressed in PAM-γ3. (B-B_1”) No GRASP signals are detected between MBON-γ3 dendrites and PPL1-γ2 axons in a wild type brain. (B_1-B_1”) is an enlarged view of the area highlighted with a dashed square in (B). (C-C1”) GRASP signals are detected between MBON-γ3 dendrites and PPL1-γ2 axons when Robo1, Robo2, and Robo3 are simultaneously knocked down in MBON-γ3 neurons. (C_1-C_1”) is an enlarged view of the area highlighted with a dashed square in (A). GRASP puncta (arrows) largely overlap with or are in close proximity of the presynaptic marker Brp-mCherry expressed in PPL1-γ2 neurons.

Deng_Fig 7

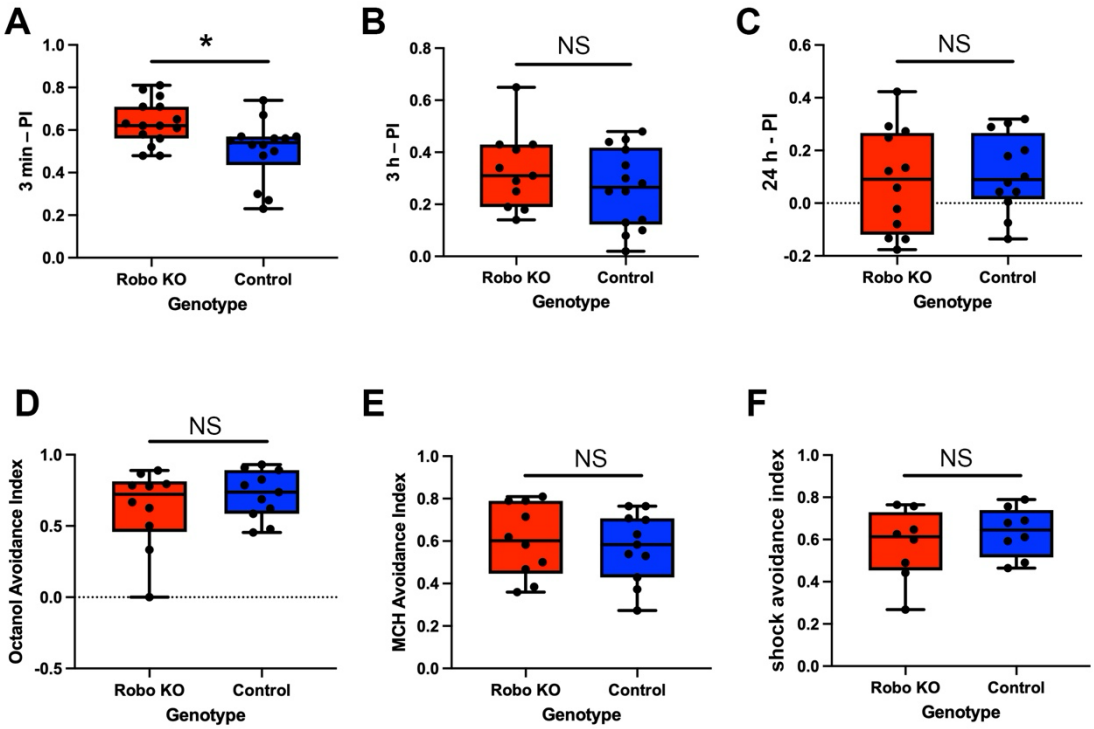
A
*
3 min – PI
1.0
0.8
0.6
0.4
0.2
0.0
Robo KO
Control
Genotype
B
NS
3 h – PI
0.8
0.6
0.4
0.2
0.0
Robo KO
Control
Genotype
C
NS
24 h - PI
0.6
0.4
0.2
0.0
-0.2
Robo KO
Control
Genotype
D
NS
Octanol Avoidance Index
1.0
0.5
0.0
-0.5
Robo KO
Control
Genotype
E
NS
MCH Avoidance Index
1.0
0.8
0.6
0.4
0.2
0.0
Robo KO
Control
Genotype
F
NS
shock avoidance index
1.0
0.8
0.6
0.4
0.2
0.0
Robo KO
Control
Genotype

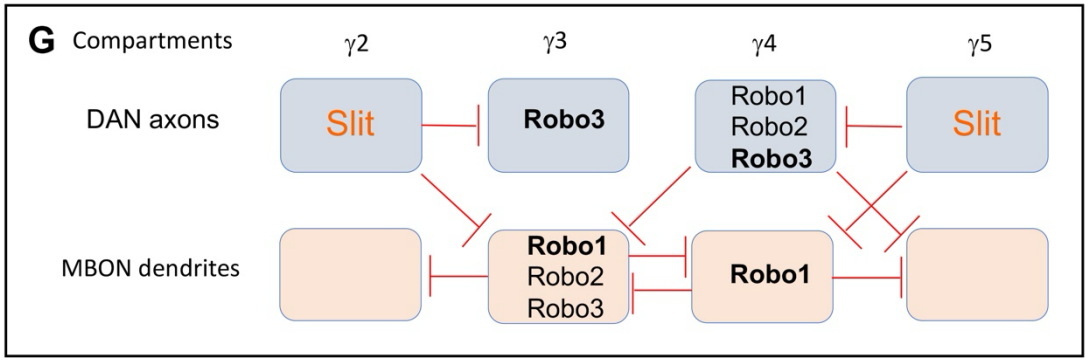
G
Compartments
γ2
γ3
γ4
γ5
DAN axons
Slit
Robo3
Robo1
Robo2
Robo3
Slit
MBON dendrites
Robo1
Robo2
Robo3
Robo1

Fig. 7. Targeting defects of MBON-γ3 dendrites affects immediate olfactory-associative memory. (A-C) Olfactory-associative memory performance index at 3 min (A), 3 hours (B), and 24 hours (C) in wild type control or Robo1 knockdown flies after conditioning. Note that the performance index at 3 min is significantly increased in Robo knockdown flies. (D-F) Robo1 knockdown flies show similar avoidance to Octanol, MCH, and electric shock before conditioning as wild type control. *, $p < 0.05$; NS, not significant, Mann-Whitney test. (G) A schematic diagram of mutual repulsive interactions (red lines) mediated by MBON dendrites or/and DAN axons between neighboring compartments. Slit is expressed in PPL1-γ2 and PAM-γ5 neurons to prevent MBON dendrites and DAN axons in the γ3 and γ4 compartments from projecting into the γ2 and γ5 compartments, respectively. MBONs and DANs in the γ3 and γ4 compartment express different Robo receptors to mediate the repulsion by Slit. The Robo receptors in bold fonts play primary roles and those in regular fonts likely play supplemental roles. In addition to PPL1-γ2 and PAM-γ5 neurons, MBON-γ3, MBON-γ4, and PAM-γ4 neurons may also repel MBON dendrites and/or DAN axons from neighboring compartments.

Deng_Supplemental_Fig S1

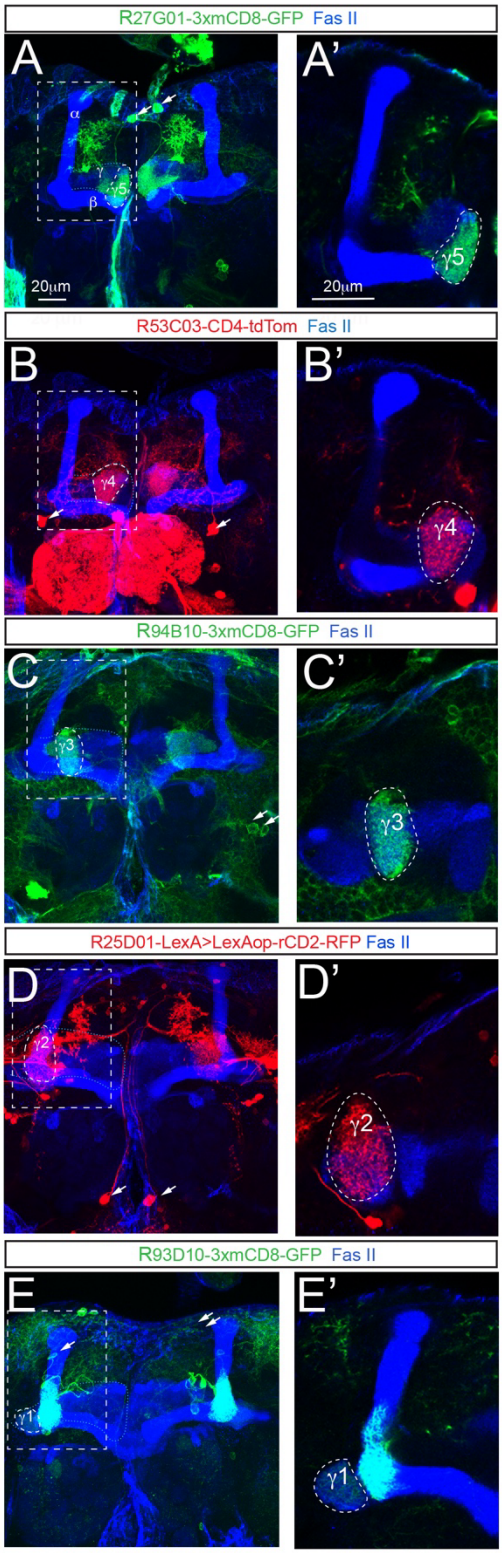

Supplemental Fig. S1. Labeling of different types of MBONs with different fluorescent markers. (A, B, C, D, E) show projected images of MBON-γ5 (A), MBON-γ4 (B), MBON-γ3 (C), MBON-γ2 (D), and MBON-γ1 (E) neurons labeled with R27G01-3xmCD8-GFP, R53C03-CD4-tdTom, R94B10-3xmCD8-GFP, LexAop-rCD2-RFP driven by R25D01-LexA, and R93D10-3xmCD8-GFP, respectively. Brains are counterstained with Fas II antibodies to labeled MB γ and α/β axonal lobes. Arrows point to the soma of MBONs. (A', B', C', D', E') show enlarged views of the areas highlighted with dashed rectangles in (A, B, C, D, E) to show dendrites of the corresponding MBONs in the respective compartments in the γ lobe in a single focal slice. Dashed circles outline the dendritic areas of individual MBONs.

Deng_Supplemental_Fig S2

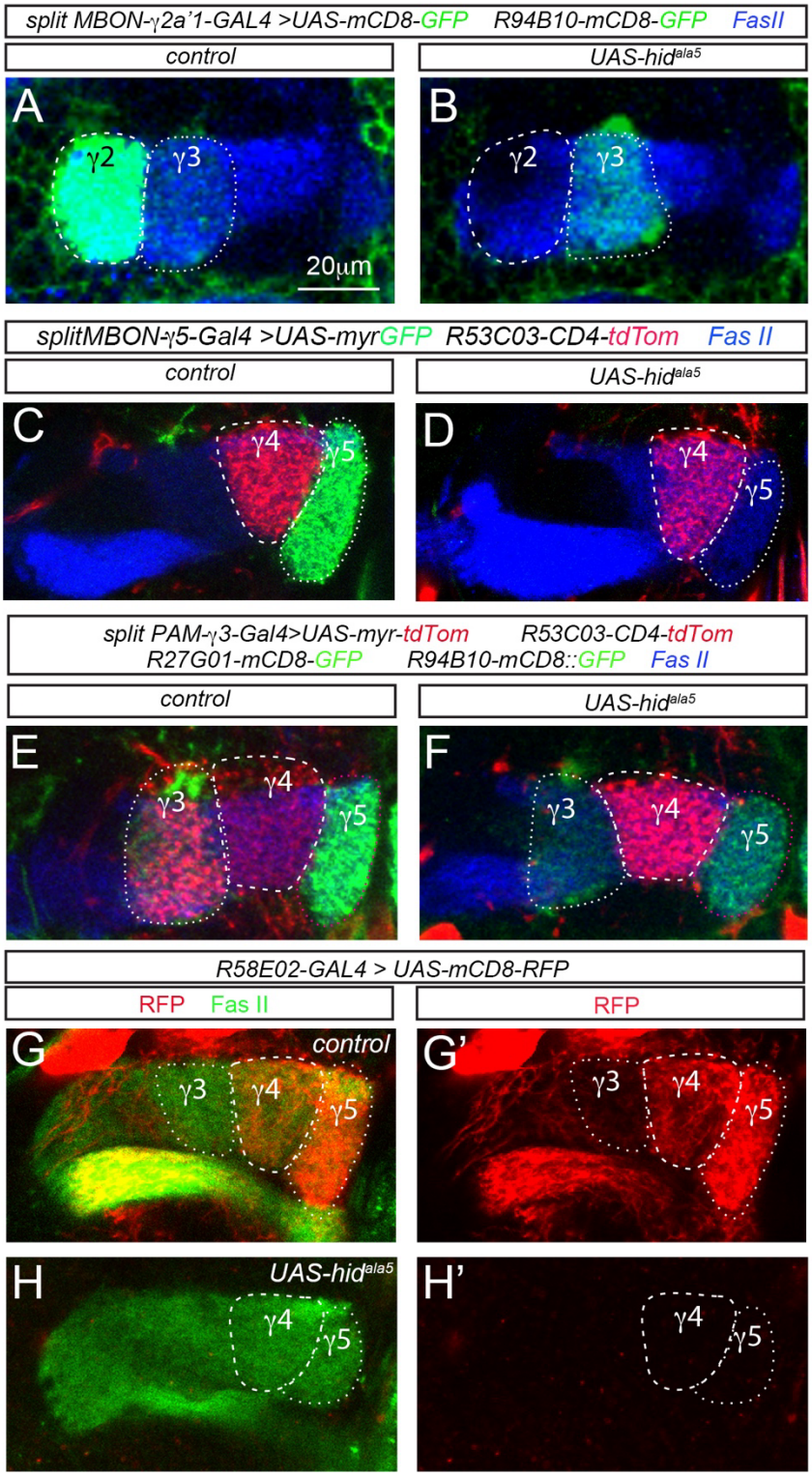

Supplemental Fig. S2. Genetic ablation of MBON-γ2, MBON-γ5, or PAM-γ3 neurons does not affect projection of MBON dendrites in neighboring compartments. (A-B) MBON-γ3 dendrites (weaker GFP, dotted circles) remain in the γ3 compartment as in the wild type brains (A) after ablation of MBON-γ2 neurons (B). Dendrites of MBON-γ2 neurons, which are labeled with stronger GFP (dashed circles) in the wild type (A), are absent in the γ2 compartment after being ablated (B). (C-D) As in wild type brains (C), MBON-γ4 dendrites (dashed circles) do not project into the γ5 compartment after ablation of MBON-γ5 neurons (D). Ablation of MBON-γ5 neurons are indicated by the loss of GFP-labeled dendrites in the γ5 compartment (dotted circles). (E-F) Projection of MBON-γ4 dendrites (dashed circle) remains similar in the presence (E) or absence (F) of PAM-γ3 neuron axons (labeled with myr-tdTom) in the γ3 compartment (white dotted circles). Projection of MBON-γ3 dendrites (weaker GFP) in the γ3 compartment is not affected by the ablation of PAM-γ3 neurons (D). MBON-γ5 dendrites are also labeled with stronger GFP in the γ5 compartment (purple circles). (G-G”) mCD8-RFP driven by R58E02-GAL4 labels PAM-γ3-5 axons in the γ3, γ4, and γ5 compartments. (H-H”) Axons of PAM-γ3-5 neurons are absent in the γ lobe after ablation. MB axonal lobes are counterstained with anti-Fas II antibodies in blue (A-F) or green (G-H”).

Deng_Supplemental_Fig S3

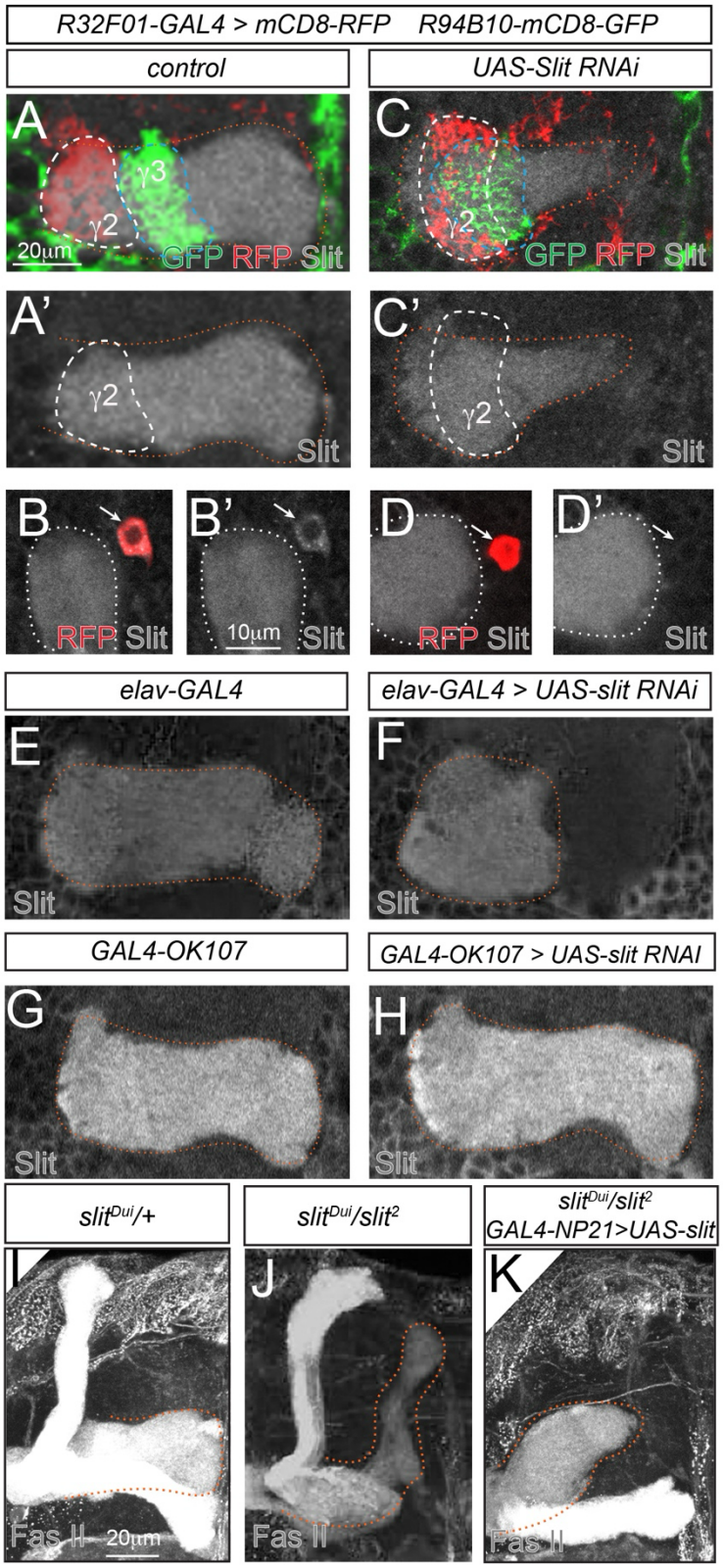

Supplemental Fig. S3. Non-specific binding of anti-Slit antibodies in the MB. (A-B') Immunostaining with anti-Slit antibodies shows staining signal in the entire MB γ lobe, including the γ2 compartment (white dashed circles) (A-A'), the MB calyx (white dotted lines) and the soma of PPL1-γ2 neurons (arrows) (B-B') in a wild type brain. PPL1-γ2 axons (white dashed circles) and MBON-γ3 dendrites (blue dashed circles) are labeled with RFP and GFP to mark the γ2 and γ3 compartments, respectively. (C-D') Expressing *UAS-slit RNAi* in PPL1-γ2 neurons does not reduce the Slit staining intensity in the γ2 compartment (C-C') but leads to projection of MBON-γ3 dendrites (GFP, blue dashed circles) in the γ2 compartment, overlapping with PPL1-γ2 axons (RFP, whit dashed circles) (C-C'), but diminishes the Slit staining signal in the soma (arrows) of PPL1-γ2 neurons (D-D'). (E-F) Pan-neuronal expression of *UAS-slit RNAi* disrupts the projection of the MB γ lobe (orange dotted circles) but does not reduce the Slit staining intensity in the γ lobe [(F), compared to the wild type control in (E)]. (G-H) Expression of *UAS-slit RNAi* in MB neurons neither disrupts the projection of the MB γ lobe (orange dotted circles) nor reduce the Slit staining intensity in the γ lobe [(H), compared to the wild type control in (G)]. (I-K) MB γ lobes project normally in $slit^{Dui}$/+ animals (I) but are mistargeted in $slit^{Dui}/slit^{2}$ mutants (J). Expression of *UAS-slit* in γ neurons does not rescue the mistargeting of the γ lobe in $slit^{Dui}/slit^{2}$ mutants (K).

Deng_Supplemental_Fig S4

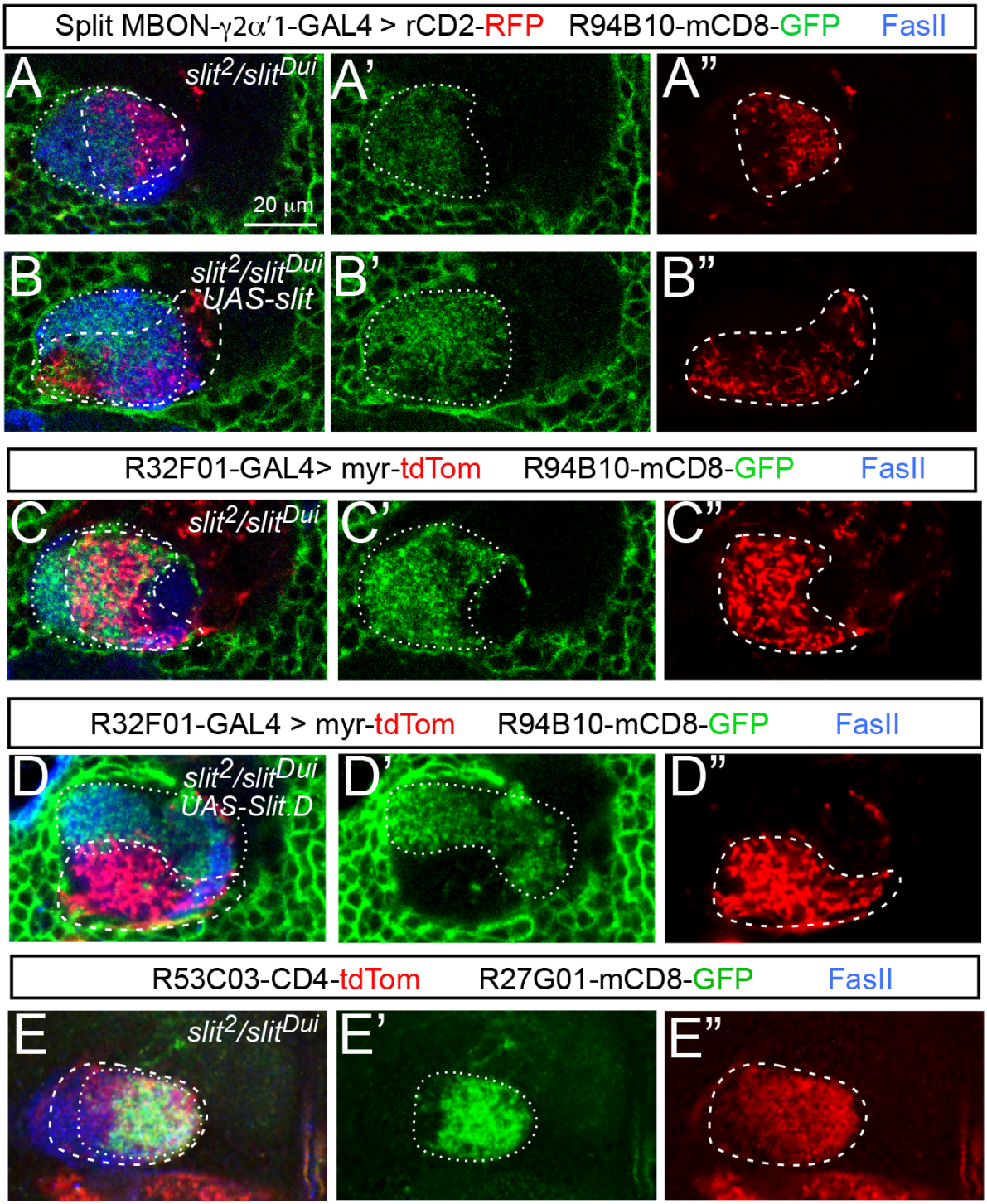

Supplemental Fig. S4. Targeting defects of dendrites of MBON-γ3 and MBON-γ4 neurons in *slit* mutants. (A-A") In a *slit*^{2}/*slit*^{Dui} mutant brain, MBON-γ3 dendrites (labeled with GFP, dotted circles) project into the γ2 compartment and overlap with MBON-γ2 dendrites (labeled with RFP, dashed circles), which are displaced from their original γ2 compartment and shift to the medial side of MBON-γ3 dendrites. (B-B") Expression of *UAS-Slit* in MBON-γ2 neurons does not restore a sharp boundary between MBON-γ3 dendrites (dotted circles) and MBON-γ2 dendrites (dashed circles) in *slit* mutants. Their dendrites remain overlap with each other. Note that MBON-γ2 dendrites are displaced from their original γ2 compartment and shift downward and medially when MBON-γ3 dendrites project into the γ2 compartment. (C-C") In a *slit*^{2}/*slit*^{Dui} mutant brain, MBON-γ3 dendrites (labeled with GFP, dotted circles) project into the γ2 compartment and overlap with PPL1-γ2 axons (labeled with RFP, dashed circles). (D-D") Expression of *UAS-Slit* in PPL1-γ2 neurons restores a sharp boundary between MBON-γ3 dendrites (dotted circles) and PPL1-γ2 axons (dashed circles) in *slit* mutants although their positions in the γ lobe are still abnormal likely due to distortion of the γ lobe in *slit* mutants. (E-E") MBON-γ4 dendrites (labeled with tdTom, dashed circles) overlap with MBON-γ5 dendrites (labeled with GFP, dotted circles) in a *slit*^{2}/*slit*^{Dui} mutant brain. In all images, brains are counterstained with Fas II antibodies to labeled MB γ and α/β lobes.